

Simple models of turbulent flows*

Stephen B. Pope^{a)}

Sibley School of Mechanical and Aerospace Engineering, Cornell University, 254 Upson Hall, Ithaca, New York 14853, USA

(Received 25 October 2010; accepted 23 November 2010; published online 18 January 2011)

Stochastic Lagrangian models provide a simple and direct way to model turbulent flows and the processes that occur within them. This paper provides an introduction to this approach, aimed at the nonspecialist, and providing some historical perspective. Basic models for the Lagrangian velocity (i.e., the Langevin equation) and composition are described and applied to the simple but revealing case of dispersion from a line source in grid turbulence. With simple extensions, these models are applied to inhomogeneous turbulent reactive flows, where they form the core of probability density function (PDF) methods. The use of PDF methods is illustrated for the case of a lifted turbulent jet flame. Lagrangian time series are now accessible both from experiments and from direct numerical simulations, and this information is used to scrutinize and improve stochastic Lagrangian models. In particular, we describe refinements to account for the observed strong Reynolds-number effects including intermittency. It is emphasized that all models of turbulence are necessarily approximate and incomplete, and that simple models are valuable in many applications in spite of their limitations. © 2011 American Institute of Physics. [doi:10.1063/1.3531744]

I. INTRODUCTION

For more than a century, researchers have been grappling with the challenges posed by turbulent flows. The research has been motivated and sustained not only by scientific curiosity and the intellectual challenges posed, but also by the ubiquity of turbulent flows in the natural world and in engineering devices, and by the importance of turbulence in enhancing the rates of transport and mixing, typically by many orders of magnitude.

There can be several different objectives in studies of turbulent flows including developing an understanding of particular flows and the processes that occur within them, developing methodologies to design engineering devices and to control the turbulent flows involved to achieve objectives such as reducing drag or promoting mixing, and—the focus of this paper—developing theories, models, and simulation techniques. The latter objective is of particular importance, as the methodologies developed often can be used to achieve the other objectives.

From the perspective of theory, modeling, and simulations, we may ask: How and when will the turbulence problem be solved? The ideal solution would be to have a tractable quantitative theory, based soundly on the underlying physics, as described by the Navier–Stokes equations. In the middle of the last century, such a solution may have seemed a realistic prospect. The theory proposed by Kolmogorov¹ in 1941 postulated that the small scales of turbulence are statistically universal and simply parametrized by the viscosity and the mean dissipation rate. If this picture were accurate,

then there would be a realistic hope for a successful statistical theory. But subsequent investigations have shown that the small scales are significantly affected by the flow-dependent large scales. It appears now that this “ideal solution” is unrealistic and unattainable. The fundamental difficulty is the nonlinear and nonlocal (in space and scale) interactions of the turbulent motions over the large range of scales present in turbulent flows.

Instead of the unattainable ideal, a realistic goal, of great practical value, is the development of tractable models and simulation approaches for the diverse range of turbulent flows encountered in engineering, oceanography, meteorology, astrophysics, and elsewhere. There is not one “turbulence problem” but a wide variety of problems of varying difficulty, dependent on the geometry of the flow and the additional processes involved (e.g., chemical reactions and multiple phases). Some of these turbulence problems have been “solved” in the sense that current models or simulations are adequately accurate for the application involved. And as progress is made over time, a greater fraction of the turbulent problems will in this sense be solved.

As the title implies, this paper focuses on *simple* models, and one of the morals (due to the statistician G. E. P. Box) is that “All models are wrong, but some are useful.” Within the turbulence research community, there is a tendency toward more complex models. All models are incomplete and inaccurate to some degree, which naturally motivates the development of increasingly more complete and more accurate models. But such advanced models are inevitably more complicated and less tractable. On the other hand, researchers and practitioners outside of turbulence research seek simple, tractable models for their turbulent flow, which may be but one aspect of their larger complex problem. There is, therefore, an important role for simple models, in spite of their flaws and limitations, and an important role for the turbu-

*This paper is based on the Otto Laporte Lecture delivered by the author on November 22, 2009, following the award of the APS Fluid Dynamics Prize at the American Physical Society Division of Fluid Dynamics Annual Meeting in Minneapolis.

^{a)}Electronic mail: s.b.pope@cornell.edu.

lence research community is to develop and understand such models.

The simple models considered here are called “stochastic Lagrangian models.” Within the turbulent flow of interest, we consider a fluid particle, i.e., a mathematical point moving with the local fluid velocity. As a function of time t , the fluid particle has position $\mathbf{X}^+(t)$, velocity $\mathbf{U}^+(t)$, acceleration $\mathbf{A}^+(t)$, and thermochemical properties $\phi^+(t)$ such as temperature and the mass fractions of chemical species. Such quantities are called Lagrangian trajectories or Lagrangian time series (when sampled at discrete times in experiments or simulations). The fluid-particle properties are, by definition, the fluid properties at the moving particle’s location. Hence, with $\mathbf{U}(\mathbf{x}, t)$ being the Eulerian velocity field, the fluid-particle velocity is

$$\mathbf{U}^+(t) = \mathbf{U}[\mathbf{X}^+(t), t]. \quad (1)$$

Stochastic Lagrangian models are stochastic processes designed to mimic the behavior of Lagrangian trajectories in turbulent flows.

In the three major sections of this paper, we examine different related aspects of stochastic Lagrangian models applied to three different flows. In Sec. II we introduce the Langevin model for velocity, and apply it to study the dispersion of heat from a line source in grid turbulence. The ideas involved go back to Langevin² and Taylor,³ and the ability of the model to describe turbulent transport (revealed through the mean temperature field) was demonstrated over 25 years ago.⁴ To study turbulent mixing (revealed through the temperature variance) we introduce a simple stochastic Lagrangian model for a conserved passive scalar. Only recently has a satisfactory model for the scalar been developed and demonstrated for the line source.^{5,6}

The simplicity of the stochastic Lagrangian models, developed by reference to dispersion in homogeneous isotropic turbulence, belies their potency. In Sec. III, we show that (with minor extensions) the same stochastic Lagrangian models lead to a complete turbulence closure for inhomogeneous turbulent reactive flows. This closure takes the form of a modeled transport equation for the joint probability density function (PDF) of velocity and composition. This PDF method, and its computational implementation as a particle/mesh Monte Carlo method, is demonstrated for the case of a lifted turbulent jet flame.

While the Langevin model is clearly very useful—as demonstrated by the results presented in Secs. II and III—a more detailed examination of its properties in Sec. IV shows that it has fundamental shortcomings and inaccuracies—“All models are wrong, but some are useful.” We describe more advanced models, which account for Reynolds-number effects⁷ and intermittency.⁸ The development of such models has been made possible by the recent investigations of Lagrangian properties using direct numerical simulations (DNS) and experiments with modern diagnostics. The paper concludes with some thoughts on the current challenges and future prospects for the modeling and simulation of turbulent flows.

This paper is intended primarily for nonspecialists, with the aim to provide an introduction to stochastic Lagrangian

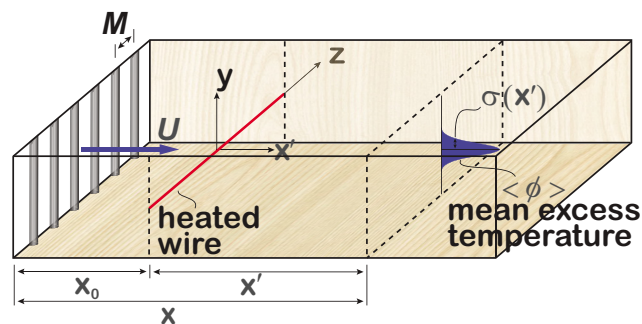


FIG. 1. (Color online) Sketch of Warhaft’s experiment on a line source in grid turbulence showing the x' - y - z -coordinate system with origin at the middle of the heated wire (which is the line source of temperature) and the (Gaussian) mean excess temperature profile of width $\sigma(x')$.

models and their use in PDF methods. The reader is encouraged to use the on-line version in order to access the animations and color figures.

II. STOCHASTIC MODELING OF TURBULENT DISPERSION

In this section, we consider one of the simplest and most basic turbulent flow problems—the dispersion of a conserved passive scalar from a line source in grid turbulence. Starting in the 1950s, there have been numerous experimental investigations of this flow:^{9–13} here we focus on that of Warhaft.¹¹ While this flow is relatively simple, it can nevertheless be used to study two of the most fundamental turbulent processes: convective transport by the turbulent velocity field and turbulent mixing.

A. Dispersion from a line source: Experimental observations

As sketched in Fig. 1, the experiment of Warhaft¹¹ was conducted in a wind tunnel in which a uniform flow passes through a turbulence-generating grid of mesh spacing M . A Cartesian coordinate system is introduced with origin at the center of the grid, with x being the direction of the mean flow, and y and z being normal to the mean flow. The mean velocity $\langle U \rangle$ is in the x -direction, while the fluctuating velocities in the x, y, z directions are denoted by u, v, w or alternatively by u_1, u_2, u_3 . To an approximation, the turbulence is isotropic, and the velocity variances decay with the downstream distance as power laws of the form

$$\frac{\langle u^2 \rangle}{\langle U \rangle^2} = A \left(\frac{x}{M} \right)^{-m}, \quad (2)$$

where A and $m=1.32$ are obtained from the measurements. At a distance x_0 downstream of the grid, a fine heated wire is stretched across the center of the wind tunnel in the z -direction (at $y=0$). The distance downstream of wire is denoted by $x' = x - x_0$, so that the coordinate system (x', y, z) has its origin in the center of the wire. The wire is sufficiently fine that it has a negligible effect on the turbulent velocity field. Because of the electrical heating of the wire, the air passing very close to the wire is heated. Thus, to an approximation, the wire is a continuous line source of heat.

To a good approximation, the (suitably normalized) temperature excess—denoted by $\phi(x', y, z, t)$ —is a conserved passive scalar.

Of interest in this flow is the behavior of the passive scalar as it is swept downstream and affected by the turbulence. Away from the side walls, statistics such as the mean $\langle \phi(x', y) \rangle$ depend solely on x' and y .

The measurements show that the lateral profiles of the mean are Gaussian, i.e.,

$$\langle \phi(x', y) \rangle = \frac{1}{\sigma(x')\sqrt{2\pi}} \exp\left(\frac{-y^2}{2\sigma(x')^2}\right), \quad (3)$$

where $\sigma(x')$ is the characteristic width of the mean profile. All theories and models predict the Gaussian shape: the challenge is to predict the downstream spreading, i.e., the dependence of $\sigma(x')$ on x' .

In the laboratory frame considered, the flow is statistically stationary and two-dimensional, with statistics varying only in the x' and y directions, and spatial gradients of statistics are dominantly in the y -direction. It is also convenient to consider a frame moving with the mean velocity. Thus, we define

$$\hat{x} = x' - \langle U \rangle t, \quad (4)$$

and consider the scalar $\phi(\hat{x}, y, z, t)$ in this frame. Now, to a good approximation, statistics depend only on y and t , and the wire (which is a continuous line source in the laboratory frame) appears as an instantaneous plane source at $y=0$, $t=0$. Thus, in this frame, the flow is decaying homogeneous isotropic turbulence (with zero-mean velocity), and the phenomenon under study is the evolution of $\phi(\hat{x}, y, z, t)$ from the initial condition of a heated plane sheet [i.e., $\phi(\hat{x}, y, z, 0) = \delta(y)$].

B. Turbulent diffusion model

The simplest models for turbulent flows are those based on the concepts of turbulent viscosity and turbulent diffusivity. The basic notion is that the mean fields in turbulent flows behave similarly to fields in laminar flows, but with enhanced “effective” viscosity and diffusivity. Specifically, the molecular diffusivity Γ is enhanced by a turbulent contribution Γ_T to yield the effective diffusivity

$$\Gamma_{\text{eff}} = \Gamma + \Gamma_T. \quad (5)$$

The turbulent diffusivity $\Gamma_T(\mathbf{x}, t)$ represents the effects of the turbulent motions, and hence can depend on the local characteristics of the turbulent velocity field. On the other hand, since the velocity field is (by definition) unaffected by passive scalars, in a consistent model, Γ_T is independent of any passive scalar field that may be present.

The most widely used turbulent viscosity model is the k - ε model,¹⁴ and it is instructive to apply it to the line source problem. In the moving frame, the flow is decaying homogeneous turbulence, for which case the k - ε model reduces to the pair of ordinary differential equations,

$$\frac{dk}{dt} = -\varepsilon, \quad (6)$$

$$\frac{d\varepsilon}{dt} = -C_{\varepsilon 2} \frac{\varepsilon^2}{k}. \quad (7)$$

Equation (6) is exact and shows that turbulent kinetic energy $k \equiv \frac{1}{2} \langle u_i u_i \rangle$ decays at a rate given by the viscous dissipation ε . Equation (7) is a model, which correctly yields the observed power law decay of the form

$$\frac{k(t)}{k(t_0)} = \left(\frac{t}{t_0}\right)^{-m}, \quad (8)$$

where the model constant $C_{\varepsilon 2}$ and the exponent m are related by

$$C_{\varepsilon 2} = \frac{1+m}{m}. \quad (9)$$

Thus, the k - ε model is successful for this simplest of turbulent flows in correctly describing the decay of the turbulence.

According to the k - ε model, the turbulent diffusivity is

$$\Gamma_T = C_\Gamma \frac{k^2}{\varepsilon}, \quad (10)$$

where C_Γ is a constant, and indeed this relation is inevitable once k and ε are taken to represent the turbulence.

In the moving frame, the exact conservation equation for the mean scalar is

$$\frac{\partial \langle \phi \rangle}{\partial t} = \frac{\partial}{\partial y} \left(\Gamma \frac{\partial \langle \phi \rangle}{\partial y} - \langle v \phi \rangle \right). \quad (11)$$

The right-hand side represents the divergence of two fluxes: that due to molecular diffusion and that due to turbulence convection. The term $\langle v \phi \rangle$ is called the (turbulent) scalar flux, and it is the covariance of the scalar and the y -direction velocity v .

The turbulent diffusion model amounts to approximating the scalar flux by

$$\langle v \phi \rangle \approx -\Gamma_T \frac{\partial \langle \phi \rangle}{\partial y}, \quad (12)$$

so that Eq. (11) becomes

$$\frac{\partial \langle \phi \rangle}{\partial t} = \frac{\partial}{\partial y} \left(\Gamma_{\text{eff}} \frac{\partial \langle \phi \rangle}{\partial y} \right). \quad (13)$$

For the homogeneous turbulence considered, Γ_T is independent of y , and varies with t as a known power law. Hence, Eq. (13) is readily solved analytically to show that the k - ε model correctly yields a Gaussian profile for $\langle \phi \rangle$, and that the predicted width $\sigma(t)$ is given by

$$\sigma(t)^2 = \int_0^t 2\Gamma_{\text{eff}}(t') dt'. \quad (14)$$

This prediction for $\sigma(t)$ is compared to the experimental data in Fig. 2 (shown in the laboratory frame). As may be seen, for small times (i.e., small x'/x_0) the model displays very significant errors and appears to be qualitatively incorrect. This is confirmed by the theory presented in Sec. II C, which also shows that the agreement between the model and the data for large times (i.e., large x'/x_0) is not fortuitous, but

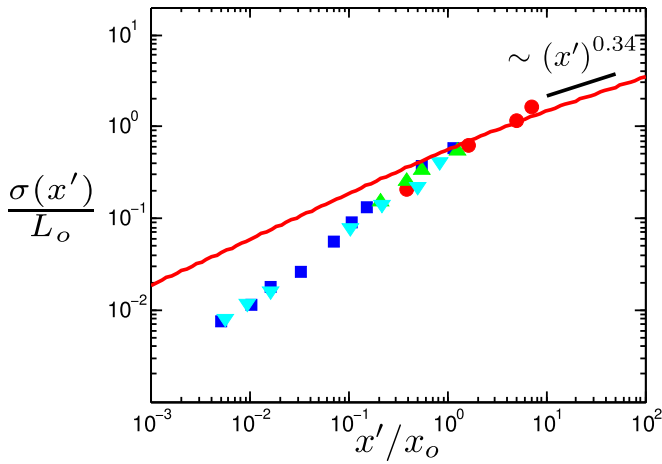


FIG. 2. (Color online) Width σ of the thermal wake (normalized by $L = k^{3/2}/\varepsilon$ at the source) against distance from the source x' normalized by the distance x_0 of the source from the grid: symbols, experimental data (Refs. 11 and 12); line, from the k - ε model.

instead the turbulent diffusion model is valid in this region.

C. Diffusion by continuous movements

Fifty years before the k - ε turbulence model, Taylor³ tackled the problem of turbulent dispersion in his famous 1921 paper “Diffusion by continuous movements.” For the line source problem, the equation governing the mean $\langle \phi \rangle$ [Eq. (11)] is derived from the instantaneous equation,

$$\frac{D\phi}{Dt} = \Gamma \nabla^2 \phi. \quad (15)$$

Taylor argued that at high Reynolds number, the molecular flux in Eq. (11) is negligible compared to the turbulent flux. With the molecular term neglected, the equation for the mean then rises from the instantaneous equation,

$$\frac{D\phi}{Dt} = 0, \quad (16)$$

i.e., the scalar ϕ is conserved following the fluid. This observation transforms the problem into that of describing the motion of fluid particles. For the line source problem in the moving frame, the mean $\langle \phi(y, t) \rangle$ is proportional to the PDF (at y, t) of the position of fluid particles originating from the source ($y=0$) at time $t=0$.

We denote by $\mathbf{X}^+(t, \mathbf{Y})$ the position at time t of the fluid particle which is at position \mathbf{Y} at time 0. By definition, the fluid particle moves with its own velocity [denoted by $\mathbf{u}^+(t, \mathbf{Y})$], which is the local Eulerian fluid velocity,

$$\frac{\partial \mathbf{X}^+(t, \mathbf{Y})}{\partial t} = \mathbf{u}^+(t, \mathbf{Y}) \equiv \mathbf{U}[\mathbf{X}^+(t, \mathbf{Y}), t]. \quad (17)$$

Focusing on the line source problem, we are interested in fluid particles which originate from $y=0$ at $t=0$, i.e., those with $Y_2=0$, and, furthermore, we are interested only in their motion in the y -direction. Consequently, we simplify the notation to consider $X^+(t)$ and $u^+(t)$ to be the y -components of position and velocity of such particles.

For given t , $X^+(t)$ is a random variable (because of the randomness of the turbulent velocity field), and we can consider its mean $\langle X^+(t) \rangle$, its variance, and its PDF. The mean is zero, since the problem is statistically symmetric about $y=0$. As mentioned, according to this theory, the mean $\langle \phi(y, t) \rangle$ is proportional to the probability density of the event $X^+(t)=y$, since $\langle \phi \rangle$ is proportional to the probability that the fluid at y, t originates from the source. In accord with experimental observations, all theories and models lead to a Gaussian PDF of $X^+(t)$, and hence to a Gaussian profile of $\langle \phi(y, t) \rangle$. The characteristic width $\sigma(t)$ of this profile is the standard deviation at $X^+(t)$,

$$\sigma(t)^2 = \langle X^+(t)^2 \rangle. \quad (18)$$

The equation for the fluid-particle motion $dX^+/dt = u^+$ can be integrated to yield

$$X^+(t) = \int_0^t u^+(t') dt', \quad (19)$$

and hence Eq. (18) can be reexpressed as

$$\sigma(t)^2 = \int_0^t \int_0^t \langle u^+(t') u^+(t'') \rangle dt' dt''. \quad (20)$$

This is Taylor’s principal result, showing that the dispersion $\sigma(t)^2$ is known in terms of the two-time Lagrangian velocity autocovariance.

Further deductions are most simply made for the case of statistically stationary turbulence (as opposed to decaying grid turbulence). In the stationary case, the autocovariance can be reexpressed as

$$\langle u^+(t') u^+(t'') \rangle = \langle u^2 \rangle \rho(|t' - t''|), \quad (21)$$

where $\langle u^2 \rangle$ is the velocity variance and $\rho(s)$ is the Lagrangian velocity autocorrelation function. DNS (Ref. 15) shows that $\rho(s)$ is well approximated by the exponential

$$\rho(s) = \exp\left(\frac{-|s|}{T_L}\right), \quad (22)$$

where T_L is the Lagrangian velocity integral time scale

$$T_L \equiv \int_0^\infty \rho(s) ds. \quad (23)$$

[The approximation equation (22) is scrutinized in Sec. IV.]

Using Eq. (21) and a nontrivial manipulation (see, e.g., Ref. 16), Eq. (20) can be reexpressed as

$$\sigma(t)^2 = 2\langle u^2 \rangle \int_0^t (t-s) \rho(s) ds. \quad (24)$$

Several important deductions (due to Taylor) can be made from Eq. (24) without invoking Eq. (22):

- (1) For very small time ($s/T_L \ll 1$), $\rho(s)$ is very close to unity, so that Eq. (24) yields

$$\sigma(t) \approx u' t, \quad \text{for } t/T_L \ll 1, \quad (25)$$

where $u' \equiv \langle u^2 \rangle^{1/2}$ is the rms velocity. This corresponds to straight-line, ballistic motion.

(2) For very large time ($t/T_L \gg 1$), Eq. (24) yields

$$\sigma(t)^2 \approx 2\langle u^2 \rangle t T_L, \quad \text{for } t/T_L \gg 1. \quad (26)$$

(3) The evolution of $\sigma(t)^2$ can be represented in terms of a time-dependent diffusivity,

$$\begin{aligned} \hat{\Gamma}(t) &\equiv \frac{d}{dt} \left(\frac{1}{2} \sigma(t)^2 \right) = \langle u^2 \rangle \int_0^t \rho(s) ds \\ &\approx \langle u^2 \rangle t, \quad \text{for } t/T_L \ll 1 \\ &\approx \langle u^2 \rangle T_L, \quad \text{for } t/T_L \gg 1. \end{aligned} \quad (27)$$

The last result establishes the validity of the turbulent diffusion model at large times with $\Gamma_T = \langle u^2 \rangle T_L$. But for smaller times, $\hat{\Gamma}(t)$ depends on the time t since the release of the source, contrary to the notion that Γ_T depends solely on properties of the turbulent velocity field.

We could proceed to obtain a prediction for $\sigma(t)$ for the line source in grid turbulence by substituting into Eq. (24) a model for the Lagrangian velocity autocovariance in decaying turbulence. But, instead, we proceed by the more powerful and general route of considering a stochastic model for $u^+(t)$.

D. The Langevin model

In an appendix to his paper,³ Taylor proposed a stochastic model for the position $X^+(t)$ of a fluid particle. According to this model, over successive small time intervals Δt , the position increments $[X^+(t+\Delta t) - X^+(t)]$ and $[X^+(t) - X^+(t-\Delta t)]$ are highly correlated. In fact, this model is identical to the stochastic model for velocity $u^+(t)$ proposed a decade earlier by Langevin² to model the velocity of a particle undergoing Brownian motion.

For the case of statistically stationary homogeneous turbulence, the Langevin model can be written as the stochastic differential equation (SDE),

$$du^+(t) = -u^+(t) \frac{dt}{T_L} + \left(\frac{2u'^2}{T_L} \right)^{1/2} dW(t), \quad (28)$$

where $W(t)$ is a Wiener process. The reader unfamiliar with SDEs can understand this equation through its finite-difference analog,

$$u^+(t+\Delta t) - u^+(t) = -u^+(t) \frac{\Delta t}{T_L} + \left(\frac{2u'^2 \Delta t}{T_L} \right)^{1/2} \xi, \quad (29)$$

where ξ is a zero-mean, unit-variance Gaussian random variable (independent for each time step). The stochastic process generated by the Langevin equation is called the Ornstein–Uhlenbeck (OU) process, which is readily analyzed (see, e.g., Ref. 16). The OU process corresponding to Eq. (28) is fully characterized by the fact that it is a continuous statistically stationary Gaussian process with mean $\langle u^+(t) \rangle = 0$, variance $\langle u^+(t)^2 \rangle = u'^2$, and exponential autocorrelation $\rho(s) = \exp(-|s|/T_L)$. The mean and variance are [by construction of Eq. (28)] consistent with the given properties of the turbulence, and, as mentioned above, the exponential autocorrelation is supported by DNS data.

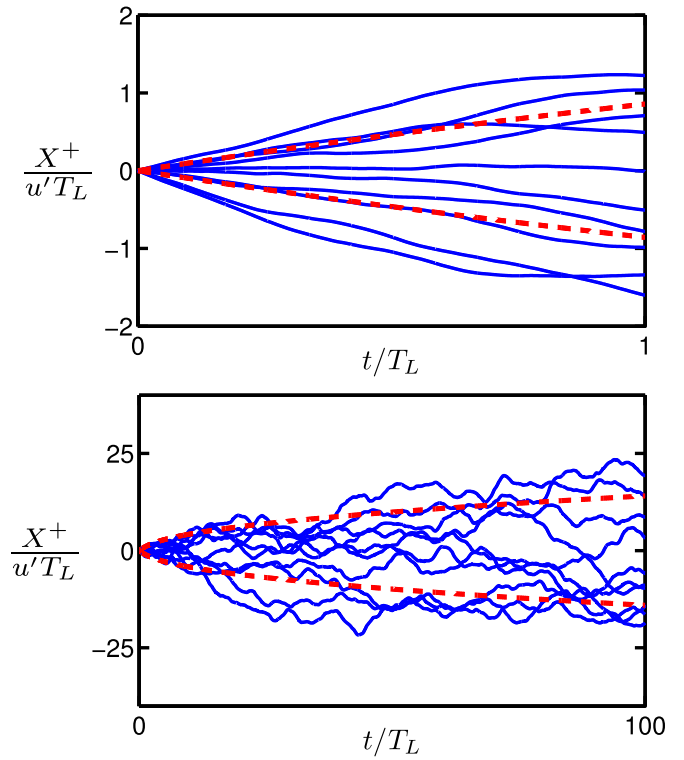


FIG. 3. (Color online) Samples of fluid-particle paths $X^+(t)$ for short times ($t/T_L \leq 1$, top) and for long times ($t/T_L \leq 100$, bottom) obtained from the Langevin model. The dashed lines show $\pm\sigma(t)$, the standard deviation of $X^+(t)$. Normalization is by the Lagrangian integral time scale T_L and the rms velocity u' .

Realizations (or sample paths) of $u^+(t)$ can be generated from Eq. (28) and then integrated to yield corresponding sample paths of $X^+(t)$. Figure 3 shows such sample paths at short times (top) and long times (bottom). The ballistic and diffusive regimes identified by Taylor are clearly evident.

In order to apply the Langevin equation to the case of decaying grid turbulence, we rewrite it as

$$du^+ = -\omega_u u^+ dt + b dW, \quad (30)$$

and we seek to relate the relaxation rate ω_u and the diffusion coefficient b to properties of the turbulence, which is characterized by the kinetic energy k and the dissipation rate ε . Two pieces of information are required to determine these two coefficients. The first is that the variance $\langle u^2 \rangle$ equals the variance of the Eulerian velocity, which (assuming isotropy) equals $\frac{2}{3}k$. Thus, the variance decays as

$$\frac{d}{dt} \langle u^2 \rangle = \frac{d}{dt} \left(\frac{2}{3}k \right) = -\frac{2}{3}\varepsilon. \quad (31)$$

The second piece of information comes from Kolmogorov¹ theory. This pertains to the second-order Lagrangian velocity structure function defined by

$$D(s) \equiv \langle [u^+(t+s) - u^+(t)]^2 \rangle, \quad (32)$$

which is simply the variance of the velocity increment over a time interval s . According to Kolmogorov, at high Reynolds number, and for s in the inertial range (i.e., $\tau_\eta \ll s \ll T_L$, where τ_η is the Kolmogorov time scale), $D(s)$ is uniquely

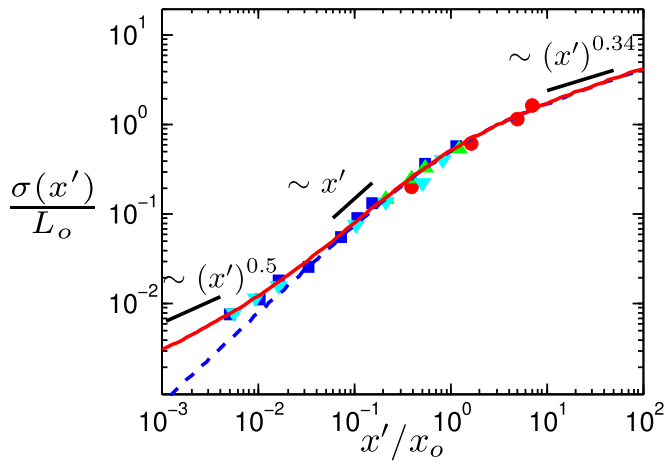


FIG. 4. (Color online) Width σ of the thermal wake (normalized by $L = k^{3/2}/\varepsilon$ at the source) against distance from the source x' normalized by the distance x_0 of the source from the grid: symbols, experimental data (Refs. 11 and 12); dashed line, from the Langevin model for fluid particles; solid line, from the Langevin model for Brownian particles.

determined by s and ε . Dimensional analysis then leads to

$$D(s) = C_0 \varepsilon s, \quad \text{for } \tau_\eta \ll s \leq T_L, \quad (33)$$

where C_0 is a universal Kolmogorov constant. (Since this relation is linear in ε , it also holds according to Kolmogorov's refined similarity hypotheses¹⁷ in the presence of intermittency.)

The Langevin equation is consistent with Eq. (33) provided that b is taken to be $(C_0 \varepsilon)^{1/2}$. Then Eq. (31) requires ω_u to be $(\frac{1}{2} + \frac{3}{4} C_0) \varepsilon / k$. Thus, for decaying turbulence, the Langevin equation can be written as

$$du^+ = - \left(\frac{1}{2} + \frac{3}{4} C_0 \right) \frac{\varepsilon}{k} u^+ dt + (C_0 \varepsilon)^{1/2} dW. \quad (34)$$

(The same equation applies to the stationary case, but with the $\frac{1}{2}$ omitted from the drift coefficient.)

The dispersion $\sigma(t)^2 = \langle X^+(t)^2 \rangle$ given by the Langevin equation (34) can be determined analytically:^{4,16} it depends solely on the decay exponent m (known from the experiment) and the constant C_0 . Figure 4 compares the experimental data for $\sigma(t)$ with the Langevin-model prediction for $C_0 = 2.1$ —the value determined by reference to these data. As may be seen, there is excellent agreement, except for very small times. This discrepancy is due to the complete neglect of molecular diffusion, which is not justified in this moderate-Reynolds-number flow ($R_\lambda \approx 50$). This deficiency is readily remedied by redefining the particles considered to be Brownian particles, moving both with the local fluid velocity and by molecular diffusion. Thus, $X^+(t)$ evolves by the SDE

$$dX^+(t) = u^+(t) dt + (2\Gamma)^{1/2} dW', \quad (35)$$

where $W'(t)$ is a Wiener process [independent of $W(t)$ in the Langevin equation]. With this modification, as may be seen from Fig. 4, the Langevin model is in excellent agreement with the data.

As indicated in Fig. 4, the theory identifies three regimes: at very early times molecular diffusion dominates and

yields $\sigma \approx \sqrt{2\Gamma t}$; at intermediate times there is ballistic turbulent motion with $\sigma \approx u' t$; and at long times there is turbulent diffusion with $\sigma \sim t^{0.34}$ —the power being less than $\frac{1}{2}$ because of the decay of the turbulence.

Comparing the poor performance of the turbulent diffusion model (Fig. 2) with the excellent performance of simple Langevin model (Fig. 4), one is reminded of Einstein's exhortation to make things as simple as possible, but no simpler. Clearly, for this simple flow, the turbulent diffusion model is too simple.

The Langevin model, in particular its short-time behavior and the specification of C_0 , is further examined in Sec. IV

E. Scalar variance

The success of stochastic Lagrangian models based on the Langevin equation to describe the mean temperature field was well established 25 years ago. Only recently, however, has the same success been achieved for the temperature variance.

For the temperature variance, which reveals the extent of turbulent mixing, there are two distinct modeling approaches. The first is based on pair dispersion in which one models the motion of a pair of Brownian particles: see Ref. 18 for a recent review. We follow the second approach in which the stochastic Lagrangian model is extended by adding composition $\phi^+(t)$ as a particle property. Furthermore, we consider particles uniformly distributed throughout the flow domain, rather than just those originally from the location of the source.

An important aspect of this approach is the estimation of mean fields from particle properties. For example, the mean scalar field (in a general flow) is obtained as

$$\langle \phi(\mathbf{x}, t) \rangle = \langle \phi^+(t) | \mathbf{X}^+(t) = \mathbf{x} \rangle, \quad (36)$$

i.e., the mean Eulerian field $\langle \phi(\mathbf{x}, t) \rangle$ is the expectation of the particle composition $\phi^+(t)$, conditional upon the particle being located at \mathbf{x} at time t . (In Sec. III C, we explain how such means are estimated in practice, in a numerical implementation of the method.)

For the case considered of a single conserved passive scalar, the simplest Lagrangian model for the scalar is the interaction by exchange with the mean (IEM) model,^{19,20}

$$\frac{d\phi^+(t)}{dt} = -\omega_m [\phi^+(t) - \langle \phi^+(t) | \mathbf{X}^+(t) \rangle], \quad (37)$$

where the composition relaxation rate ω_m is taken to be

$$\omega_m = \frac{1}{2} C_\phi \frac{\varepsilon}{k}, \quad (38)$$

where C_ϕ is a model constant. Thus, according to this IEM model, the particle composition $\phi^+(t)$ relaxes to the local mean $\langle \phi^+(t) | \mathbf{X}(t) \rangle$ at the rate ω_m .

Despite its apparent simplicity, the line source in grid turbulence contains features that are challenging to over-simple models, and the IEM model is found to be deficient in predicting the variance. Close to the heated wire, the instantaneous structure of the temperature field is that of an unsteady laminar thermal wake that is flapped around by the

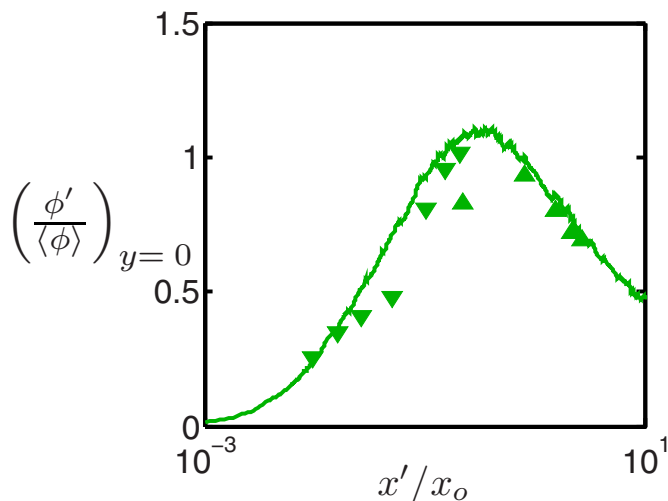


FIG. 5. (Color online) Axial profile of the ratio of the rms temperature fluctuation to the mean temperature excess on the centerline downstream of the line source: symbols, experimental data (Ref. 11); line, calculations using the IECM model (Ref. 6).

turbulent motions. As a consequence, in this early region, the direct effects of molecular diffusion to broaden the thermal wake are important, and the temperature field is highly correlated with the velocity (in the y -direction).

A refined model⁶ which accounts for these effects is given by

$$\begin{aligned} \frac{d\phi^+(t)}{dt} = & -\omega_m[\phi^+(t) - \langle \phi^+(t) | X^+(t), u^+(t) \rangle] \\ & + \Gamma \frac{\partial^2 \langle \phi^+(t) | X^+(t), u^+(t) \rangle}{\partial y^2}. \end{aligned} \quad (39)$$

The term in ω_m is similar to the IEM model, but now the relaxation is to the mean conditioned on the particle velocity (in addition to its position). This part is called the interaction by exchange with the conditional mean (IECM) model.^{21–23} The term in Γ implements the direct effects of molecular diffusion in the evolution of the composition, instead of through a random walk in the position equation, Eq. (35). Analysis shows that while the use of Brownian particles, Eq. (35), is valid for studying the mean $\langle \phi \rangle$, it introduces a spurious source of composition variance.

Figures 5 and 6 show axial and radial profiles of the normalized rms temperature fluctuations ϕ' for Warhaft's line source experiment. As may be seen, there is excellent agreement between the model calculations and the measurements. The calculations are obtained from the stochastic Lagrangian model for fluid particles ($dX^+/dt = u^+$), in which the velocity $u^+(t)$ evolves by the Langevin equation [Eq. (34)], and the composition $\phi^+(t)$ evolves by the IECM model [Eq. (39)].

This stochastic Lagrangian model has been applied to the ingenious experiment by Warhaft¹¹ on pairs of line sources. Instead of a single heated wire at $x'=0, y=0$, there are two wires, separated by a distance d_0 , located at $x'=0, y = \pm \frac{1}{2}d_0$. Conceptually, and in the modeling, we can consider the two wires to be sources of different conserved pas-

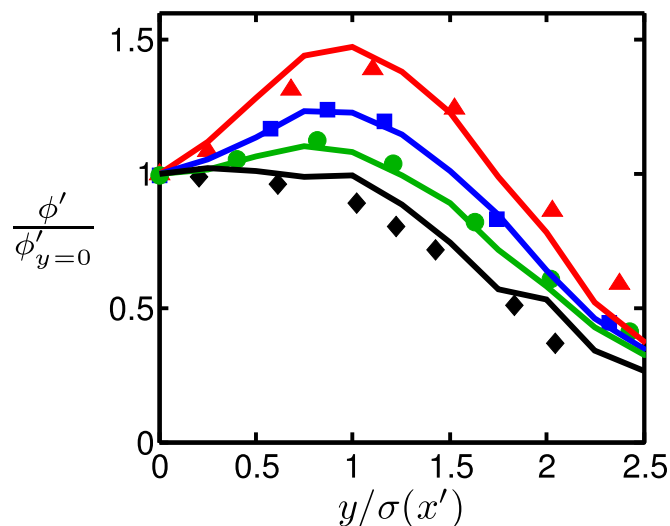


FIG. 6. (Color online) Radial profiles of the rms temperature fluctuation normalized by its centerline value at axial locations (from top to bottom) $x'/M=0.36, 0.62, 1.0, 100$: symbols, experimental data (Ref. 11); line, calculations using the IECM model (Ref. 6).

sive scalars, denoted by ϕ_1 and ϕ_2 . As functions of x' and y , in addition to the means $\langle \phi_1 \rangle$ and $\langle \phi_2 \rangle$, and variances $\langle \phi_1'^2 \rangle$ and $\langle \phi_2'^2 \rangle$, we can consider the covariance $\langle \phi_1' \phi_2' \rangle$ and the correlation coefficient

$$\rho_{12} \equiv \frac{\langle \phi_1' \phi_2' \rangle}{[\langle \phi_1'^2 \rangle \langle \phi_2'^2 \rangle]^{1/2}}. \quad (40)$$

The covariance and the correlation coefficient are important quantities, as they reveal the rate of mixing of different scalars, which is clearly relevant to reactive flows. In the experiment, Warhaft deduced the covariance using a superposition principle based on three separate measurements of the temperature variance: one with the wire at $y = \frac{1}{2}d_0$ heated, one with the wire at $y = -\frac{1}{2}d_0$ heated, and one with both wires heated.

Figure 7 shows the axial evolution of the correlation coefficient ρ_{12} on the centerline ($y=0, z=0$) for different wire separations d_0 . As may be seen, this evolution is highly nontrivial and strongly dependent on the value of d_0 . The stochastic Lagrangian model is completely successful in representing these observations.

III. PROBABILITY DENSITY FUNCTION METHODS

With straightforward modifications and extensions, the simple stochastic Lagrangian models for position, $X^+(t)$, velocity, $u^+(t)$, and composition, $\phi^+(t)$, can be used to produce a closed modeled equation for inhomogeneous turbulent flows, including reacting flows. Specifically, the models provide a closure for the transport equation for the one-point, one-time Eulerian joint PDF of velocity and composition. In practice, this modeled PDF equation is solved by a particle/mesh Monte Carlo method, the core of which is a large number of particles, each evolving according to the stochastic Lagrangian models.

In this section, this PDF method is described, along with its associated particle-mesh method, and its application to a

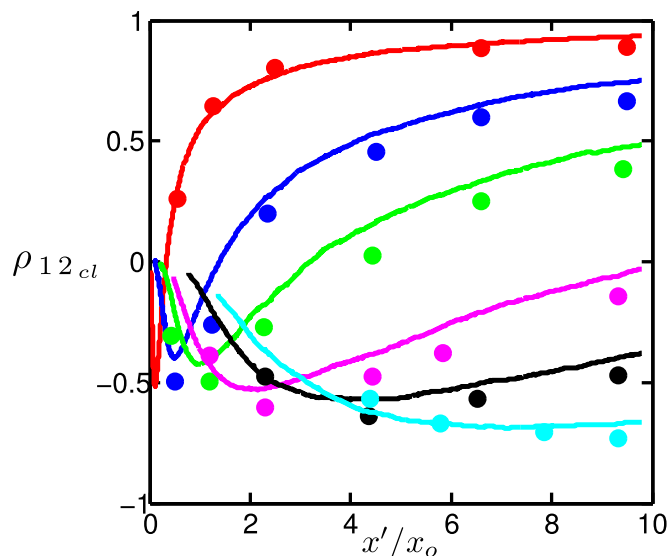


FIG. 7. (Color online) Axial profiles on the centerline of the correlation coefficient between the scalars from a pair of line sources: symbols, experimental data (Ref. 11); lines, calculations using the IECM model (Ref. 6). The separation between the sources is (from top to bottom downstream) $d_0 = 1.2, 8, 14, 25, 35$ mm.

turbulent lifted jet flame. First, we contrast the Eulerian statistical approach and the stochastic Lagrangian approach for obtaining turbulence closures.

A. Eulerian statistical and stochastic Lagrangian approaches

1. The Eulerian statistical approach

The Eulerian statistical approach, which goes back to Reynolds' paper,²⁴ consists of the following stages:

- (1) The starting point is the set of exact, instantaneous conservation equations for the flow variables considered.
- (2) We then derive the exact (but unclosed) equations governing a chosen set of statistics (e.g., means, variances), which are called “knowns.”
- (3) We provide models for other statistics arising in these equations (referred to as “unknowns”) in terms of the knowns.
- (4) The result is a set of closed, modeled equations for the knowns.

As a simple example, we consider a constant-property flow involving a single reactive scalar $\phi(\mathbf{x}, t)$, whose conservation equation is

$$\frac{D\phi}{Dt} = \left(\frac{\partial}{\partial t} + \mathbf{U} \cdot \nabla \right) \phi = \Gamma \nabla^2 \phi + S(\phi), \quad (41)$$

where $\mathbf{U}(\mathbf{x}, t)$ is the Eulerian velocity field, Γ is the molecular diffusivity, and S is the chemical source term, which is a known, highly nonlinear function of the local value of ϕ .

In the simplest “mean flow” closure, the set of statistics considered consists of the mean velocity $\langle \mathbf{U} \rangle$, the mean pressure $\langle p \rangle$, and the mean scalar $\langle \phi \rangle$. Conservation equations for $\langle \mathbf{U} \rangle$ and $\langle p \rangle$ —the Reynolds equations—are derived from the

Navier–Stokes equations; but here we focus on the mean composition equation obtained from Eq. (41), which is

$$\left(\frac{\partial}{\partial t} + \langle \mathbf{U} \rangle \cdot \nabla \right) \langle \phi \rangle = \nabla \cdot (\Gamma \nabla \langle \phi \rangle - \langle \mathbf{u} \phi \rangle) + \langle S(\phi) \rangle, \quad (42)$$

where the Reynolds decomposition has been used to express the velocity as

$$\mathbf{U} = \langle \mathbf{U} \rangle + \mathbf{u}. \quad (43)$$

In Eq. (42), since $\langle \mathbf{U} \rangle$ and $\langle \phi \rangle$ are knowns, the left-hand side and the term in Γ are in “closed form,” i.e., they are known in terms of the knowns. The remaining quantities—the scalar flux $\langle \mathbf{u} \phi \rangle$ and the mean source term $\langle S(\phi) \rangle$ —are unknowns for which models or closure approximations are required. The simplest model for the scalar flux is a turbulent diffusion model (as discussed above) which is

$$\langle \mathbf{u} \phi \rangle \approx -\Gamma_T \nabla \langle \phi \rangle, \quad (44)$$

where Γ_T is the turbulent diffusivity (which is obtained through an additional model). At this level of closure, the only information about the composition is its mean $\langle \phi \rangle$. Hence, for the mean source term, the only available closure approximation is

$$\langle S(\phi) \rangle \approx S(\langle \phi \rangle). \quad (45)$$

While this relation is exact if $S(\phi)$ is a linear function, for the highly nonlinear functions encountered in combustion, for example, this approximation can be in error by orders of magnitude. With the models [Eqs. (44) and (45)] substituted into the exact mean equation [Eq. (42)], we obtain the final result—the closed, modeled conservation equation,

$$\left(\frac{\partial}{\partial t} + \langle \mathbf{U} \rangle \cdot \nabla \right) \langle \phi \rangle = \nabla \cdot ([\Gamma + \Gamma_T] \nabla \langle \phi \rangle) + S(\langle \phi \rangle). \quad (46)$$

This Eulerian statistical approach, described here for the means, can be applied to means, variances, and covariances (to yield a “second-moment” closure) or to higher statistics. In particular, it can be applied to the Eulerian one-point one-time joint PDF of velocity and composition. This quantity, denoted $f(\mathbf{V}, \psi; \mathbf{x}, t)$, is the joint probability density of the event $\{\mathbf{U}(\mathbf{x}, t) = \mathbf{V}, \phi(\mathbf{x}, t) = \psi\}$, where \mathbf{V} and ψ are the corresponding sample-space variables. In this case, the unknowns to be modeled are conditional statistics, such as the conditional diffusion

$$\mathcal{D}(\mathbf{V}, \psi; \mathbf{x}, t) = \langle \Gamma \nabla^2 \phi | \mathbf{U} = \mathbf{V}, \phi = \psi \rangle. \quad (47)$$

2. The stochastic Lagrangian approach

In the stochastic Lagrangian approach, we select a set of fluid properties to be considered. For definiteness, we consider the velocity \mathbf{U} and composition ϕ . As in the Eulerian statistical approach, the starting point is the instantaneous conservation equations for the quantities considered. In the case considered, these are the Navier–Stokes equations for $\mathbf{U}(\mathbf{x}, t)$,

$$\frac{D\mathbf{U}}{Dt} = -\frac{1}{\rho} \nabla p + \nu \nabla^2 \mathbf{U}, \quad \nabla \cdot \mathbf{U} = 0 \quad (48)$$

(where ρ and ν are the constant density and kinematic viscosity and $p(\mathbf{x}, t)$ is the pressure), and Eq. (41) for $\phi(\mathbf{x}, t)$. The end result of the approach is a closed modeled conservation equation for the one-point, one-time Eulerian joint PDF of the properties considered; here $f(\mathbf{V}, \psi; \mathbf{x}, t)$, the velocity-composition joint PDF.

We consider the joint PDF f to be “known” and hence any quantity that can be deduced from f is also a known. Consequently, moments such as $\langle \mathbf{U} \rangle$, $\langle \phi \rangle$, $\langle u_i u_j \rangle$, $\langle u_i \phi \rangle$ are known, as is the mean pressure field $\langle p \rangle$, since it can be obtained from a Poisson equation of known source.

The second step in the stochastic Lagrangian approach is to write down the fluid-particle evolution equations, which follow directly from the Eulerian conservation equations. Thus, for the case considered, the fluid-particle properties $\mathbf{X}^+(t)$, $\mathbf{U}^+(t)$, $\phi^+(t)$ evolve by

$$\frac{d\mathbf{X}^+}{dt} - \mathbf{U}^+(t) = 0, \quad (49)$$

$$\frac{d\mathbf{U}^+}{dt} + \left[\frac{1}{\rho} \nabla \langle p \rangle \right]^+ = \left[-\frac{1}{\rho} \nabla p' + \nu \nabla^2 \mathbf{U} \right]^+, \quad (50)$$

$$\frac{d\phi^+}{dt} - S(\phi^+(t)) = (\Gamma \nabla^2 \phi)^+, \quad (51)$$

where $[]^+$ indicates that the quantity is evaluated at $(\mathbf{x}, t) = [\mathbf{X}^+(t), t]$. These equations are written with known terms on the left-hand side and unknown terms on the right. As mentioned, the mean pressure $\langle p \rangle$ is known, whereas the pressure function p' is unknown.

In addition to statistics deduced from the joint PDF, the knowns include the fluid-particle properties. Hence, importantly, the source term $S[\phi^+(t)]$ is known directly in terms of the particle composition.

In the statistical Eulerian approach, the unknowns to be modeled are statistics which, in statistically stationary flows, are independent of time. In contrast, in the stochastic Lagrangian approach, the unknowns [the right-hand sides of Eqs. (50) and (51)] are time-dependent random processes. The right-hand side of Eq. (50) is the random force due to the fluctuating pressure gradient and viscous stresses, whereas the right-hand side of Eq. (51) represents the rate-of-change of composition due to molecular diffusion.

The third stage in the stochastic Lagrangian approach is to provide models—either stochastic or deterministic—for the unknown random processes. Thus, using the IEM model, Eq. (51) is modeled as

$$\frac{d\phi^+}{dt} - S[\phi^+(t)] = -\omega_m [\phi^+(t) - \langle \phi \rangle^+], \quad (52)$$

where ω_m is the turbulent mixing rate (specified by another aspect of the modeling) and $\langle \phi \rangle^+$ is the mean composition at the particle location. Similarly, using the Langevin equation to model the random force, Eq. (50) is modeled as

$$d\mathbf{U}^+ + \left[\frac{1}{\rho} \nabla \langle p \rangle \right]^+ dt = -\omega_u [\mathbf{U}^+ - \langle \mathbf{U} \rangle^+] dt + (C_0 \varepsilon)^{1/2} d\mathbf{W}, \quad (53)$$

where again the relaxation rate ω_u and the mean dissipation rate ε are specified as another aspect of the modeling. The determination of ω_m , ω_u , and ε is discussed in Sec. III B. Note that for the inhomogeneous flows considered, the appropriate drift term in the Langevin equation causes \mathbf{U}^+ to relax to the local mean velocity. Also, if the effects of mean diffusion and mean viscous stresses are important, then these terms (which are known) can be included.

The final stage is to derive from the model particle equations a modeled conservation equation for the joint PDF $f(\mathbf{V}, \psi; \mathbf{x}, t)$. By design, this equation is closed.

3. Comparison of approaches

A significant difference between the Eulerian and Lagrangian approaches is in the form of the quantities to be modeled. In the Eulerian approach, it is statistics which require modeling, and their complexity increases with the level of closure considered. In the stochastic Lagrangian approach, to be modeled are the instantaneous, time-dependent physical processes affecting the fluid-particle properties. Thus, the modeling is very direct.

A second-moment closure and a PDF model can be compared in terms of the processes requiring modeling. To this end, we rewrite the governing equations as

$$\frac{\partial \mathbf{U}}{\partial t} + (\langle \mathbf{U} \rangle + \langle \mathbf{u} \rangle) \cdot \nabla \mathbf{U} + \frac{1}{\rho} \nabla \langle p \rangle = \nu \nabla^2 \mathbf{U} - \frac{1}{\rho} \nabla p', \quad (54)$$

$$\frac{\partial \phi}{\partial t} + (\langle \mathbf{U} \rangle + \langle \mathbf{u} \rangle) \cdot \nabla \phi - \boxed{S(\phi)} = \Gamma \nabla^2 \phi. \quad (55)$$

In both approaches, the processes represented by the terms on the right-hand side require modeling (although their means are in closed form in both approaches). In the PDF approach, all the processes represented by the terms on the left-hand side are in closed form and do not require modeling. In contrast, in a second-moment closure, the terms in boxes—representing convection by the turbulent velocity and the chemical source term—do need to be modeled.

B. Joint PDF of velocity, composition, and turbulent frequency

For application to turbulent reactive flows, the stochastic Lagrangian models and PDF methods described above are generalized and extended in three ways.^{25,26} First, the single composition variable $\phi^+(t)$ is replaced by a set of n_ϕ composition variables $\phi^+(t)$, which completely describe the thermochemical composition of the fluid. For low-Mach-number flows involving n_s chemical species, typically $\phi^+(t)$ is taken to be the n_s species mass fractions and the enthalpy (or temperature); as far as the thermochemistry is concerned, the pressure is adequately represented by its mean at a reference location (usually atmospheric pressure). For high-speed flows, the pressure needs to be included as an additional

variable.²⁷ Second, the “turbulent frequency” $\omega^+(t)$ is added as a (modeled) property of a fluid particle.^{16,28} Roughly, $\omega^+(t)$ can be thought of as the instantaneous dissipation rate $\varepsilon^+(t)$ divided by the local turbulent kinetic energy k , so that $\langle \omega^+ \rangle$ corresponds to the quantity $\omega = \varepsilon/k$ in the k - ω model, and, similarly, $k\langle \omega^+ \rangle$ corresponds to ε in the k - ε model. This turbulent frequency is added to the model in order to determine the relaxation rates ω_u and ω_m (appearing in the Langevin and IEM models) and the mean dissipation rate ε [appearing in the diffusion term of the Langevin model, Eq. (53)]. A stochastic process is used to model the evolution of $\omega^+(t)$.^{16,28}

Third, the assumption of constant density is removed. In its place there is an equation of state giving the density $\rho^+(t)$ of the fluid particle as a function of its composition $\phi^+(t)$ (and of the pressure).

The result is a set of stochastic Lagrangian models for the fluid-particle properties: $\mathbf{X}^+(t)$, $\mathbf{U}^+(t)$, $\phi^+(t)$, and $\omega^+(t)$. From these one can deduce a closed modeled conservation equation for the velocity-composition-frequency joint PDF, $\tilde{f}(\mathbf{V}, \psi, \eta; \mathbf{x}, t)$, where \mathbf{V} , ψ and η are the sample-space variables corresponding to \mathbf{U}^+ , ϕ^+ and ω^+ .

Thus, the simple stochastic models for fluid-particle properties lead to a general and powerful result: a single closed modeled equation for the joint PDF \tilde{f} , describing inhomogeneous turbulent reactive flows.

C. Particle/mesh method

In order for the modeled PDF equation to be useful, we need methods for its solution. Only for the simplest of cases in homogeneous turbulence are analytical solutions feasible; and, inevitably, for inhomogeneous flows, numerical methods are required. The PDF equations present an insurmountable challenge to conventional grid-based methods because of the high dimensionality of the PDF. For example, for a statistically stationary and two-dimensional flow involving just three chemical species, the joint PDF $\tilde{f}(V_1, V_2, V_3, \psi_1, \psi_2, \psi_3, \psi_4, \eta; x_1, x_2)$ is ten-dimensional. Even with an extremely coarse grid with ten nodes in each direction, 10^{10} grid nodes are required, which is challenging, to say the least.

The most widely used method to solve the PDF equations is a particle/mesh method,^{25,29} outlined below, which is based directly on the stochastic Lagrangian models. Other methods that have been developed (especially for the composition PDF) include grid-based particle methods,³⁰ stochastic field methods,^{31,32} and approximate methods based on the direct quadrature method of moments (DQMOM).³³

We illustrate the operation of the particle/mesh method for the highly simplified case (sketched in Fig. 8) of a statistically stationary and two-dimensional lifted turbulent flame. There is a central plane jet of cold fuel and hot quiescent air on each side. As shown in the sketch, a rectangular solution domain is selected and covered by a uniform Cartesian mesh.

The fundamental representation of the flow is in terms of a large number N of computational particles, which model fluid particles (on different realizations of the flow). At time t , the n th particle has the following properties: position

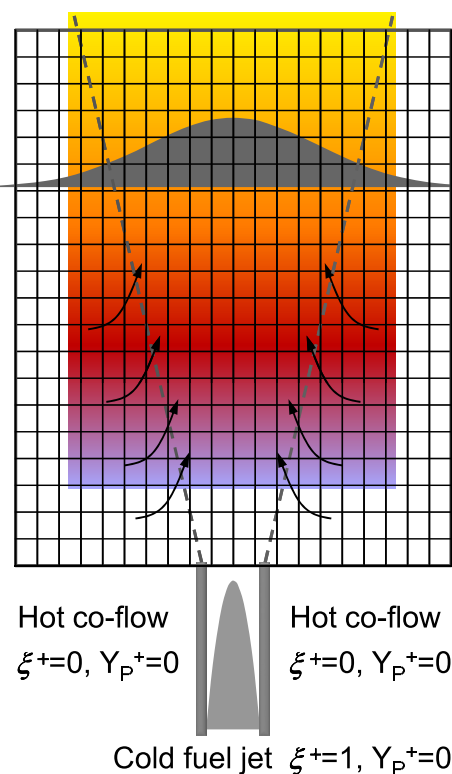


FIG. 8. (Color online) Sketch of a highly simplified, plane, lifted flame formed from a cold fuel jet issuing into hot quiescent air. Also shown are the domain and the mesh used in the particle/mesh method.

$X_1^{(n)}(t)$, $X_2^{(n)}(t)$; velocity $U_1^{(n)}(t)$, $U_2^{(n)}(t)$, $U_3^{(n)}(t)$; frequency $\omega^{(n)}(t)$; and composition $\phi_1^{(n)}(t)$, $\phi_2^{(n)}(t)$. In this highly simplified illustration, the two composition variables are taken to be mixture fraction ξ and the product mass fraction Y_p , i.e., $\{\phi_1^{(n)}(t), \phi_2^{(n)}(t)\} = \{\xi^{(n)}(t), Y_p^{(n)}(t)\}$. The particle properties evolve in time according to stochastic Lagrangian models. The particles move with their own velocity, which evolves by the Langevin equation. The compositions evolve by the IEM model, and the mass fraction of product increases due to a chemical source term.

Figure 9 shows the motion of the particles and (via color coding) their mixture fraction (left) and product mass fraction (right). As may be seen, particles emanate from the jet exit, and particles in the coflow are entrained into the jet. New particles enter at the side boundaries of the domain, and particles exit at the downstream boundary. The (expected) number density of the particles is uniform: this is a consequence of the uniform number density of the initial particle distribution and of the inflowing particles, and of the mean continuity equation ($\nabla \cdot \langle \mathbf{U} \rangle = 0$, for this constant-density flow).

The particles entering the domain from the jet have $\xi^{(n)} = 1$, $Y_p^{(n)} = 0$, while those in the coflow have $\xi^{(n)} = 0$, $Y_p^{(n)} = 0$. The intermediate values of $\xi^{(n)}$ (i.e., $0 < \xi^{(n)} < 1$) arise solely due to the IEM mixing model (because mixture fraction is a conserved scalar and so has no chemical source term). The chemical source of product $S(\xi, Y_p)$ is appropriately specified to be zero for $\xi = 0$ (pure air) and for $\xi = 1$ (pure fuel). Hence, mixing to intermediate values of ξ pre-

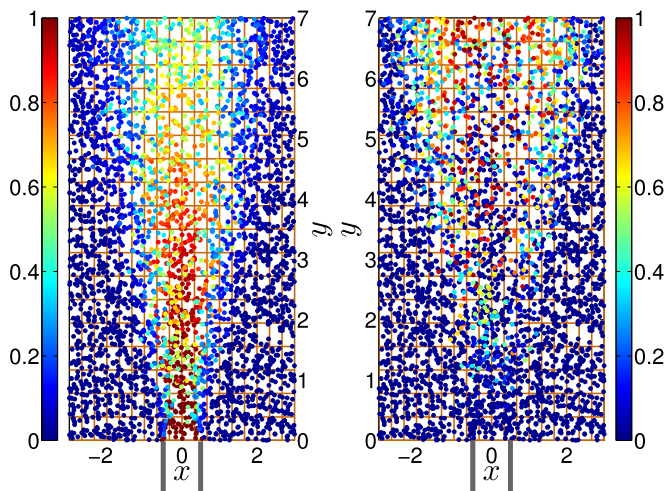


FIG. 9. (Color online) Scatter plots of particles in the x - y solution domain for the lifted jet flame. The particles are grayscale-coded (color-coded online) by mixture fraction (left) and by product mass fraction (right) (enhanced online). [URL: <http://dx.doi.org/10.1063/1.3531744.1>]

cedes reaction, and consequently significant values of $Y_p^{(n)}$ are observed only downstream of $y \approx 1$, corresponding approximately to the base of the lifted flame.

Several important observations can be made about the ensemble of particles within a given mesh cell, for example, a cell around $x=0$, $y=4$, in the center of the flame. First, it is possible for two particles to have the same position but significantly different velocity and composition. This is because the computational particles model fluid particles on *different* realizations of the flow. For the same reason, it is not possible to extract two-point turbulence statistics from the particles. Second, within a cell there is a distribution of particle properties, reflecting the distribution of fluid properties in the turbulent flow: in the particle/mesh method, the PDF is not represented directly, but the joint PDF of particle properties within a cell models the same joint PDF in the turbulent flow. Third, ensemble averages of properties (e.g., \mathbf{U}^+ , ϕ^+ , ω^+) of particles within a cell provide estimates of the corresponding means (i.e., $\langle \mathbf{U} \rangle$, $\langle \phi \rangle$, $\langle \omega \rangle$) at cell centers.

Figure 10 illustrates that instantaneous cell means contain significant statistical fluctuations, which are here larger than normal because of the relatively small number of particles used in this simple simulation. However, as illustrated in the right-hand frame, for this statistically stationary flow, the statistical fluctuations can be reduced at will by time averaging to yield stable estimates of means.

The stochastic Lagrangian models governing the particles' evolution contain both particle properties [$\mathbf{X}^+(t)$, $\mathbf{U}^+(t)$, $\phi^+(t)$, $\omega^+(t)$] and also means evaluated at particle locations (e.g., $\langle \mathbf{U} \rangle^+$, $\langle \phi \rangle^+$). In particle/mesh methods, the mesh is used in mean estimation (most simply by ensemble averaging over cells) and also in the interpolation of means onto the particles (most simply by multilinear interpolation). In practice, more sophisticated techniques may be used for mean estimation and for interpolation.³⁴

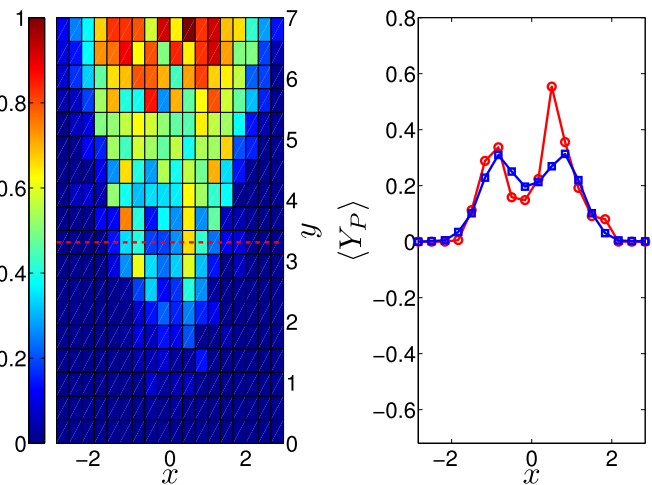


FIG. 10. (Color online) Cell means of product mass fraction obtained from the particle/mesh method applied to the simple lifted flame. Left: contour plot of instantaneous cell means. Right: lateral profile at $y \approx 3.2$ of the instantaneous [circles (red)] and time-averaged [squares (blue)] cell mean (enhanced online). [URL: <http://dx.doi.org/10.1063/1.3531744.2>]

D. Application to turbulent flames

As described above, the particle/mesh method, based on stochastic Lagrangian models, amounts to a numerical solution to the modeled joint PDF transport equation. Based on this approach, there have been numerous PDF-method studies of turbulent flames, which have recently been reviewed by Haworth.²⁶ Among the demonstrated successes of the approach^{35,36} is its ability to account quantitatively for the local extinction and reignition observed in the Sandia series of piloted jet diffusion flames.³⁷ Here, we illustrate the performance of the PDF method for the single case of a lifted jet flame in a heated coflow—a laboratory flame, qualitatively similar to that considered in Sec. III C. The flame considered^{38–40} consists of a central fuel jet (of diameter D) of an H_2/N_2 mixture at 300 K surrounded by a hot coflow consisting of the products of lean H_2 /air combustion at temperature T_c around 1000 K. A striking observation is that the lift-off height H of the flame increases rapidly as the coflow temperature is decreased in the narrow range from 1010 to 1050 K.

PDF calculations of this flame have been performed by Cao *et al.*⁴¹ and Wang and Pope⁴² using the method described above, based on the particle/mesh method and stochastic models for velocity, composition, and frequency. The 11 composition variables are the enthalpy and ten chemical species, which react according to a detailed chemical mechanism.⁴³ Figure 11 compares the measured and calculated normalized lift-off height H/D as a function of coflow temperature. As may be seen, there is excellent agreement (especially considering the ± 25 K experimental uncertainty in the absolute temperature). The calculated profiles of mean and rms temperature and species⁴¹ are also in excellent agreement with the experimental data.

Insight into the flame stabilization mechanism can be gained by examining particle properties in the PDF calculations. Specifically, we examine the evolution of the particles' mixture fraction $\xi^+(t)$ and temperature $T^+(t)$ as they move up

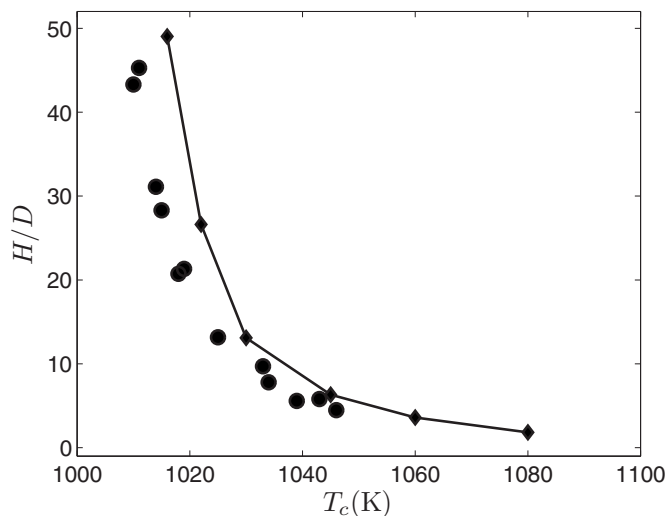


FIG. 11. Lift-off height H (normalized by the jet diameter D) against coflow temperature T_c : symbols, experimental data (Ref. 39); line with symbols, PDF calculations (Ref. 41).

in the flame. Figure 12 shows the ξ - T composition space. Pure fuel and pure coflow correspond to the points $(\xi, T) = (1, 300 \text{ K})$ and $(\xi, T) = (0, 1045 \text{ K})$, respectively. If there were inert mixing between these two streams, then all particles would lie on the line between these two points (labeled “inert mixing”). On the right-hand part of this line, the temperatures are low, and the mixture is essentially inert. In contrast, on the left-hand part of the line, the temperatures are sufficiently high for the mixture to autoignite. The most reactive mixture—that with the shortest ignition-delay time—occurs at a quite lean mixture, $\xi \approx 0.07$. If the particles reacted to the point of reaching chemical equilibrium, then they would lie on the indicated upper curve.

Figure 13, from the PDF calculations of Wang and Pope,⁴² shows the evolution of the properties of particles that emanate from the fuel jet. Hence, initially, all of the particles

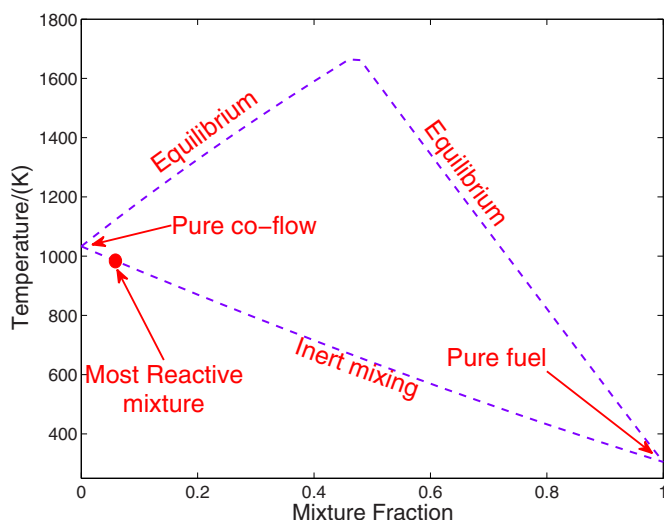


FIG. 12. (Color online) The composition space (projected onto the mixture fraction/temperature plane) for the Cabra lifted flame, showing compositions corresponding to pure fuel, pure coflow, inert mixing, and chemical equilibrium.

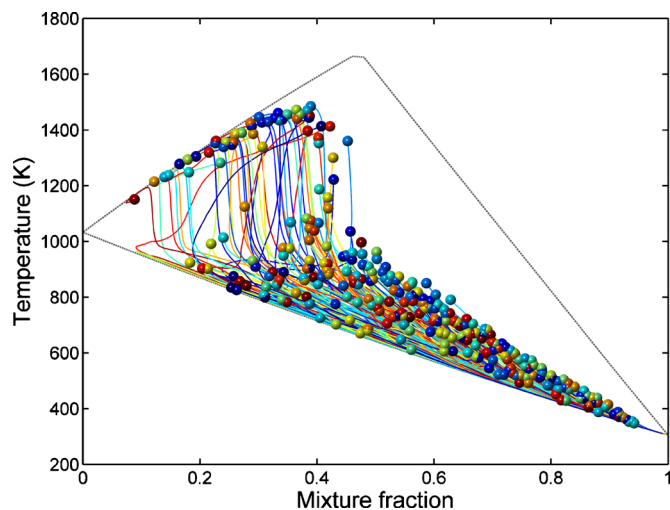


FIG. 13. (Color online) Scatter plot of mixture fraction and temperature of particles emanating from the fuel jet in PDF calculations (Ref. 42) of the Cabra flame. Print version, particles at $x/D=13$; on-line version, animation with time corresponding to x/D (enhanced online). [URL: <http://dx.doi.org/10.1063/1.3531744.3>]

are close to $(\xi, T) = (1, 300 \text{ K})$. As time evolves, the particles move upward [increasing $X_1^+(t)$], and the animation shows the particle properties evolving as their axial position increases. That is, “time” in the animation corresponds to downstream distance x/D . As may be seen in the animation, early on ($x/D < 9$) there is essentially inert mixing. At $x/D \approx 9$, a few particles approach the most reactive composition and then move upward, away from the inert-mixing line, by virtue of chemical reactions. As more particles react, mixing increases the temperature of other particles until they are sufficiently hot ($T \geq 1000 \text{ K}$) to react at a significant rate. Eventually, nearly all of the particles are close to the equilibrium line, and they move along it due to mixing.

The picture that emerges from these PDF calculations is that the route to flame stabilization is inert mixing of the fuel and coflow leading to mixtures that autoignite and then propagate the combustion. In contrast to most other flames, this stabilization mechanism does not require propagation of heat or products against the flow. Subsequent studies^{44,45} have confirmed and amplified this view.

E. Large-eddy simulation/PDF methods

In the PDF method described above, the velocity-frequency joint PDF provides a statistical description of the flow and turbulent motions of all scales. Over the past two decades, large-eddy simulation (LES) has emerged as a popular alternative to purely statistical approaches. In LES, the large-scale turbulent motions are explicitly represented, while statistical models account for the influence of the unresolved, smaller scales. The statistical models for the small scales are usually simple algebraic models—for example, the Smagorinsky model—but PDF methods are also used.

In the LES context, there are nontrivial issues concerned with the appropriate definition of the PDF (or related quantity). Based on the filtering approach to LES, Pope⁴⁶ introduced the filtered density function (FDF). The corresponding

governing equations have been derived,⁴⁷ modeled, and implemented.⁴⁸ However, the FDF pertains to a single realization and does not account for the distribution of subfilter-scale fields. In the author's view, a better definition is that of a PDF conditional on the resolved fields, as proposed by Fox³³ and developed by Pope.⁴⁹ At this stage of development, the difference between LES/FDF and LES/PDF is purely conceptual, with the modeled equations used being the same. However, there are real differences in their exact evolution equations, especially in the molecular transport terms as the LES is refined to approach DNS, and we can expect modeled LES/PDF equations to be developed to conform to this known limiting behavior.

There are several different PDF approaches, dependent on the set of variables considered, primarily combinations of composition, velocity, and frequency. Most of these approaches have been implemented in the LES context by Givi and co-workers.⁵⁰ However, the most widely used LES/PDF approach is for reactive flows, and it uses conventional LES modeling for the velocity field, and the PDF approach for the compositions. In this case, the position $\mathbf{X}^+(t)$ of the computational particles evolves by the SDE

$$d\mathbf{X}^+(t) = \left[\tilde{\mathbf{U}} + \frac{1}{\langle \rho \rangle} \nabla \Gamma_T \right]^+ dt + \sqrt{\left(\frac{2\Gamma_T}{\langle \rho \rangle} \right)^+} d\mathbf{W}, \quad (56)$$

where $\tilde{\mathbf{U}}(\mathbf{x}, t)$ is the resolved LES velocity field, $\langle \rho \rangle$ is the resolved density, and Γ_T is the turbulent (subgrid-scale) diffusivity.

In recent years, there has been an increasing use of LES/PDF methods for turbulent combustion, both in academic research and in industry.⁵¹ Reviews of this work are provided by Pitsch,⁵² Haworth,²⁶ and Haworth and Pope,⁵³ and there are recent examples using a particle/mesh method,⁵⁴ using the stochastic fields method⁵⁵ and using DQMOM.⁵⁶ While LES/PDF is computationally more expensive than both LES and PDF methods, it combines the merits of both in providing an accurate description of the turbulent velocity field and of the turbulence-chemistry interactions, which typically occur on the smallest, unresolved scales.

F. Discussion on the modeling of mixing in PDF and LES/PDF methods

Models are sometimes criticized for lacking a representation of a physical process deemed essential to the phenomenon at hand. Clearly, in reactive flows, the processes of molecular diffusion and thermal conductivity are essential, since only by molecular diffusion can fuel and oxidant mix to form a reactive mixture, and only by conduction can hot and cold fluids produce warm fluid. It is these processes that in PDF methods are modeled by the IEM and similar models. It is interesting to observe, therefore, that PDF methods are successful in accounting for challenging phenomena such as local extinction and reignition, and stabilization of lifted flames in hot coflows, and yet these models do not involve the molecular diffusivity or conductivity of the fluid. Instead, in accord with the cascade picture of turbulence, the *rate* of

molecular mixing is modeled to be determined by the large-scale turbulent motions, independent of the molecular properties. Given that the Reynolds numbers of the turbulent flames mentioned are not large, it is perhaps surprising how successful this scaling argument appears to be.

In spite of the successes mentioned above, it is certainly the case that the modeling of molecular mixing is not satisfactory in all respects, and many attempts have been made to construct improved models, e.g., Refs. 57–59. Perhaps the greatest challenge is posed by premixed turbulent combustion in the flamelet regime. In that case, the steepest scalar gradients result from a reaction-diffusion balance in the flamelets, rather than from the straining-diffusion balance experienced by nonreactive scalars. In several studies,^{60,61} PDF methods have been applied to premixed combustion in the flamelet regime.

There are two interesting observations concerning molecular diffusion in LES/PDF. First, in contrast to PDF methods, the direct effect of molecular diffusion can be significant, and even dominant. In LES simulations of the Sandia Flame D, it is found that (on reasonable grids) the molecular diffusivity is larger than the turbulent diffusivity in the near field and at all but the lowest temperatures.⁶² (This observation is relevant to all LES approaches, not just to LES/PDF.)

To make the second observation, we consider a high-Reynolds-number flow involving the mixing of a conserved scalar ϕ , the mixture fraction, which is zero in one stream and unity in the other. The integral scale of the turbulence is L , and the LES resolution parameter (e.g., the filter width) Δ is in the inertial range ($L \gg \Delta \gg \eta$).

With $\bar{\phi}$ denoting the LES field, and with $\langle \rangle$ denoting the mean, the scalar can be decomposed as

$$\phi = \langle \bar{\phi} \rangle + (\bar{\phi} - \langle \bar{\phi} \rangle) + (\phi - \bar{\phi}). \quad (57)$$

The three terms on the right-hand side correspond to the mean, the resolved fluctuation, and the residual fluctuation. To a good approximation, the composition variance can be expressed as the sum of resolved and residual contributions,

$$\langle (\phi - \langle \phi \rangle)^2 \rangle \approx \langle (\bar{\phi} - \langle \bar{\phi} \rangle)^2 \rangle + \langle (\phi - \bar{\phi})^2 \rangle. \quad (58)$$

Standard scaling arguments¹⁶ give the residual variance decreasing as $(\Delta/L)^{2/3}$ as Δ decreases, and hence this modeled contribution becomes small compared to the known resolved contribution. This is the normal picture of LES—the modeled unresolved contributions become progressively less important as Δ decreases.

Consider now the composition $\phi^+(t)$ of a computational particle in a LES/PDF calculation of this flow. For the case considered ($\Delta \gg \eta$), the direct effects of molecular diffusion are negligible (since $\Gamma \ll \Gamma_T$), whereas molecular mixing is modeled, for example, by the IEM model. We observe, therefore, that $\phi^+(t)$ evolves solely due to the modeled term: if the mixing model were omitted, then there would be no mechanism for $\phi^+(t)$ to depart from its initial value (0 or 1), and hence the predicted composition PDF would be a double-delta function everywhere. Furthermore, scaling arguments

show that the (normalized) mixing rate ω_m increases as $(\Delta/L)^{-2/3}$, indicating that in some sense the “strength” of the model increases as Δ decreases. Nevertheless, since the residual variance decreases as Δ decreases, the sensitivity of the LES/PDF calculations to the model also decreases.

IV. ADVANCED STOCHASTIC LAGRANGIAN MODELS

In this section, we examine more closely the Lagrangian velocity in homogeneous isotropic turbulence, and the extent to which it is described by the Langevin model. Referring to Box’s statement, “All models are wrong; but some are useful,” we have already seen the usefulness of the Langevin model not only for isotropic turbulence, but as an important component of PDF methods applied to inhomogeneous flows such as turbulent flames. Nevertheless, when examined in detail, the model is found to be wrong—or, more charitably, it provides an incomplete description of the phenomena. In Secs. IV A–IV D that follow, we examine the Lagrangian velocity on small time scales, observe deficiencies of the Langevin model, and show how they can be remedied.

Prior to 1989, we had little detailed knowledge of Lagrangian statistics in turbulence due to the obvious experimental difficulties. However, over the past 20 years, starting with the work of Yeung and Pope,¹⁵ we have obtained extensive, detailed information from DNS;^{63–65} and in the past decade, remarkable progress has been made in experimental techniques enabling the measurement of Lagrangian velocity and acceleration.^{66–69} It is this information from DNS and experiments which has enabled the development of more advanced stochastic Lagrangian models.

A. Lagrangian velocity increments

We consider statistically stationary, homogeneous, isotropic turbulence with turbulence intensity u' and mean dissipation rate ε . A component of the Lagrangian velocity (of a fluid particle) is denoted by $u^+(t)$. This has mean zero and variance u'^2 . The most basic multitime statistics are the autocorrelation function

$$\rho(s) \equiv \langle u^+(s)u^+(0) \rangle, \quad (59)$$

and the second-order Lagrangian structure function

$$D(s) \equiv \langle [u^+(s) - u^+(0)]^2 \rangle, \quad (60)$$

which is just the variance of the increment over the time interval $s \geq 0$. These two functions are related to each other by

$$D(s) = 2u'^2(1 - \rho(s)). \quad (61)$$

According to the Langevin model, the structure function is

$$D(s) = C_0 \varepsilon T_L (1 - e^{-s/T_L}), \quad (62)$$

where the Lagrangian velocity integral time scale T_L is related to the Eulerian turbulence properties by

$$T_L = \frac{2u'^2}{C_0 \varepsilon} = \frac{4k}{3C_0 \varepsilon}. \quad (63)$$

Note that for small times ($s/T_L \ll 1$), Eq. (62) yields

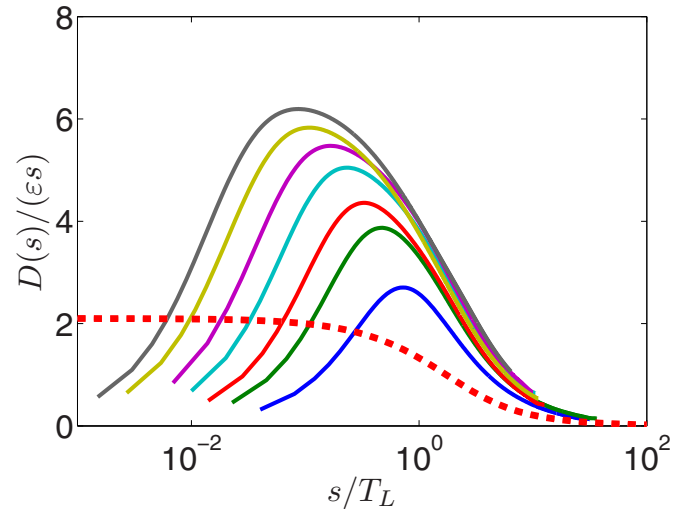


FIG. 14. (Color online) Compensated second-order Lagrangian structure functions: solid lines, DNS (Ref. 70) at Reynolds numbers (from bottom to top) $R_\lambda = 43, 86, 140, 235, 393, 595, 1000$; dashed line, Langevin model with $C_0 = 2.1$.

$$D(s) \approx C_0 \varepsilon s, \quad \text{for } \frac{s}{T_L} \ll 1, \quad (64)$$

consistent with the Kolmogorov hypotheses.

Figure 14 shows compensated structure functions, i.e., $D(s)/(\varepsilon s)$, obtained from DNS,⁷⁰ for Taylor-scale Reynolds numbers R_λ from 43 to 1000, compared to the Langevin-model result, Eq. (62). The following clear observations can be made from the DNS data:

- (1) There is a strong Reynolds-number dependence. Indeed, it is generally found that compared to Eulerian statistics, Lagrangian statistics exhibit a stronger Reynolds-number dependence, and do so up to higher Reynolds numbers.
- (2) Even at the highest Reynolds number, $D(s)/(\varepsilon s)$ does not convincingly display the plateau predicted by Kolmogorov theory [Eq. (64)].
- (3) At larger times [for s to the right of the peak of $D(s)/(\varepsilon s)$] there is a collapse of the compensated structure functions at different Reynolds number (when plotted against s/T_L).
- (4) At very small times, $D(s)/(\varepsilon s)$ increases linearly with s , since a Taylor series for $[u^+(s) - u^+(0)]$ yields

$$D(s) \approx s^2 \left\langle \left(\frac{du^+}{dt} \right)^2 \right\rangle, \quad \text{for } \frac{s}{\tau_\eta} \ll 1. \quad (65)$$

In comparison, the Langevin model has no Reynolds-number dependence, it does yield a plateau, and this extends to $s = 0$. [Note that $u^+(t)$ given by the Langevin equation is continuous but not differentiable, and so Eq. (65) does not apply to it.]

B. Reynolds number

It is straightforward to incorporate Reynolds-number dependence in the Langevin model simply by making the

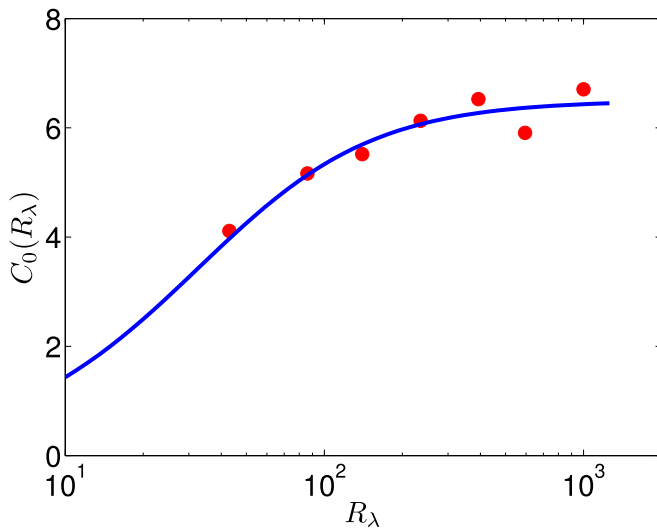


FIG. 15. (Color online) The Langevin-model constant C_0 against Reynolds number: symbols, from DNS (Ref. 70) and Eq. (67); line, empirical fit, Eq. (68).

model coefficient C_0 depend on R_λ , i.e., $C_0(R_\lambda)$. Consistency with the Kolmogorov hypotheses requires only

$$\lim_{R_\lambda \rightarrow \infty} C_0(R_\lambda) = C_0, \quad (66)$$

where now we distinguish between the Kolmogorov constant C_0 and the model coefficient $C_0(R_\lambda)$. Furthermore, $C_0(R_\lambda)$ can be determined directly from DNS data via Eq. (63), i.e.,

$$C_0 = \frac{4k}{3\varepsilon T_L}. \quad (67)$$

Figure 15 shows values of C_0 thus obtained from DNS,⁷⁰ compared to the empirical fit

$$C_0(R_\lambda) = \frac{6.5}{(1 + 140R_\lambda^{-4/3})^{3/4}}, \quad (68)$$

which is based on a suggestion by Sawford *et al.*⁷¹ As may be seen, the fit represents the data well, and is consistent with the Kolmogorov hypotheses with $C_0=6.5$.

Figure 16 compares the compensated structure functions from DNS with those from the Langevin model with $C_0(R_\lambda)$ specified by Eq. (67). As may be seen, the Langevin model now provides an accurate representation of the structure function for $s/\tau_\eta > 10$, say. Even though C_0 is specified based on the data, this agreement for the structure function is not inevitable. Instead, it indicates that, except in the dissipation range ($s < 10\tau_\eta$), $D(s)$ is characterized by the single time scale T_L .

C. Stochastic model for acceleration

As observed from Fig. 16, the behavior of the Langevin model is qualitatively incorrect at small times. This is inevitable given that $u^+(t)$ is modeled as a diffusion process. The problem can be removed, however, by moving the stochastic modeling to the next level; that is, by constructing a stochastic model for the Lagrangian acceleration $a^+(t)$, and then obtaining the velocity from $du^+/dt = a^+$.

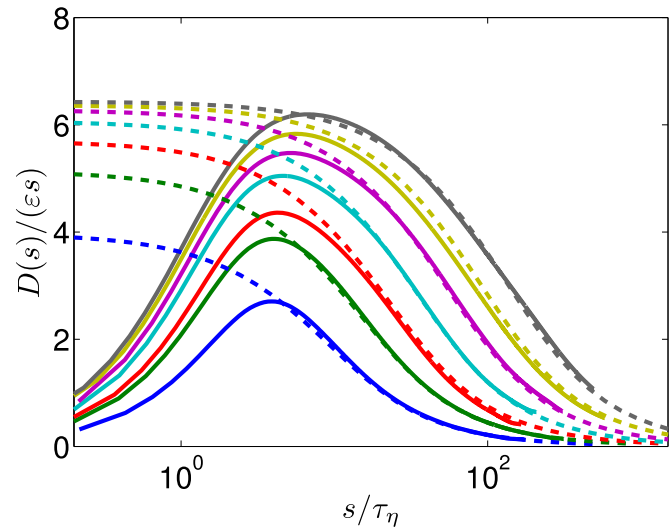


FIG. 16. (Color online) Compensated second-order Lagrangian structure functions: solid lines, DNS (Ref. 70) at Reynolds numbers (from bottom to top) $R_\lambda=43, 86, 140, 235, 393, 595, 1000$; dashed lines, Langevin model with C_0 obtained from Eq. (67).

In 1991, Sawford⁷ introduced a linear stochastic model for acceleration,

$$da^+ = - \left(1 + \frac{\tau}{T_\infty} \right) \frac{a^+}{\tau} dt - \frac{u^+}{T_\infty \tau} dt + \left\{ 2a'^2 \left(\frac{1}{\tau} + \frac{1}{T_\infty} \right) \right\}^{1/2} dW. \quad (69)$$

The two specified time scales T_∞ and τ are related to the integral scale and the Kolmogorov scale, respectively, and their ratio increases with Reynolds number. Based in these time scales and the rms velocity u' , the acceleration scale is defined by

$$a'^2 = \frac{u'^2}{T_\infty \tau}. \quad (70)$$

Analytic expressions for the autocorrelation functions and structure functions can be deduced from Sawford's model. Figure 17 compares the predicted compensated structure functions with those from DNS. As may be seen, there is good agreement, and in particular the small time scales are well represented.

D. Intermittency

As is to be expected, the statistics of acceleration and velocity increments over small time intervals are found to be highly non-Gaussian—a manifestation of interval intermittency. For example, in an experiment at $R_\lambda=680$, Mordant *et al.*⁷² measured the kurtosis of acceleration to be greater than 100, compared to the Gaussian value of 3. From the DNS of Yeung *et al.*,⁷³ Fig. 18 shows the PDF of acceleration. As may be seen, this is much broader than the Gaussian distribution (of the same standard deviation).

As originally suggested by Oboukhov⁷⁴ and Kolmogorov¹⁷ in 1962, the standard way to approach internal intermittency is to condition statistics based on the local

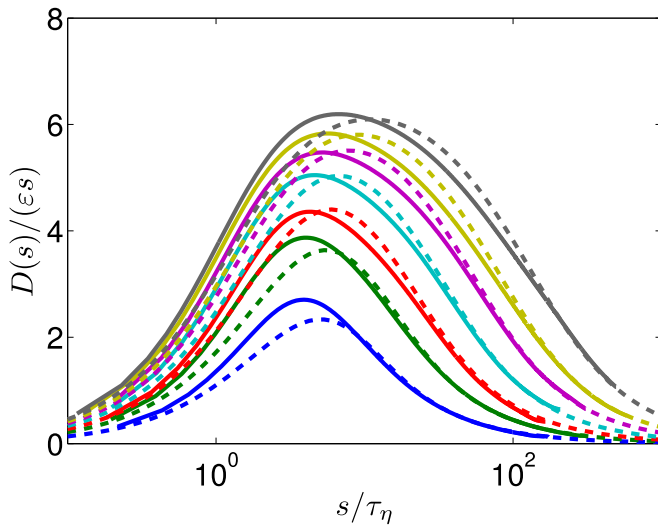


FIG. 17. (Color online) Compensated second-order Lagrangian structure functions: solid lines, DNS (Ref. 70) at Reynolds numbers (from bottom to top) $R_\lambda=43, 86, 140, 235, 393, 595, 1000$; dashed lines, from Sawford’s model (Ref. 7), Eq. (69).

dissipation rate. An early lesson from DNS (Ref. 15) is that, for this purpose, the pseudodissipation $\varphi \equiv \nu \partial u_i / \partial x_j \partial u_i / \partial x_j$ is superior to the dissipation $\varepsilon \equiv \frac{1}{2} \nu (\partial u_i / \partial x_j + \partial u_j / \partial x_i) \times (\partial u_i / \partial x_j + \partial u_j / \partial x_i)$.

Also shown in Fig. 18 are the PDFs of acceleration conditional on φ . Specifically, there are five conditional PDFs corresponding to the five quintiles of φ . As may be seen, the conditional PDFs are much narrower than the unconditional PDF, and, remarkably, they are essentially independent of the conditioning variable, i.e., the five curves collapse.

Several stochastic models have been constructed which account for intermittency.^{8,75,76} The starting point is a stochastic model for pseudodissipation, $\varphi^+(t)$. A striking observation from DNS is that the one-time PDF of φ^+ is very close

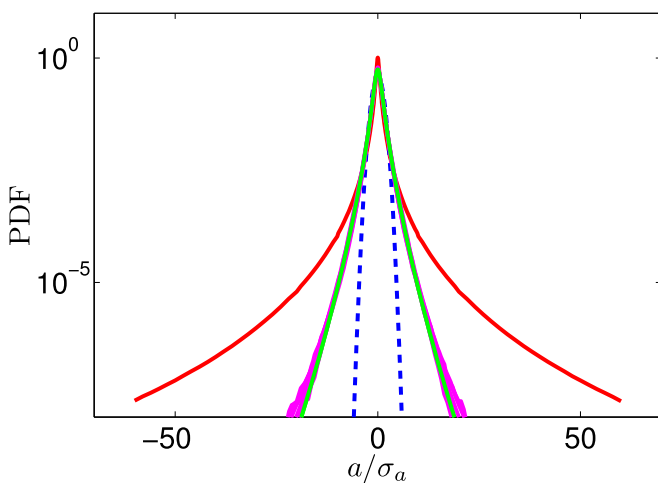


FIG. 18. (Color online) Standardized PDFs of acceleration from DNS (Ref. 73): outer solid line (red), unconditional PDF; inner solid lines (six indistinguishable lines), PDFs conditional on pseudodissipation quintiles (magenta, online), and the cubic Gaussian equation [Eq. (73)] (green, online); inner dashed line, Gaussian (blue).

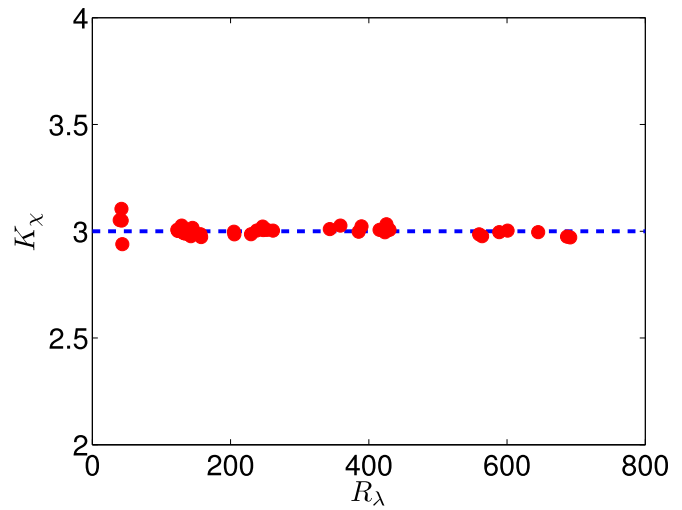


FIG. 19. (Color online) Kurtosis of χ , the logarithm of pseudodissipation, obtained from DNS (Ref. 73) against Reynolds number compared to the Gaussian value of 3.

to log-normal, or, equivalently, the quantity

$$\chi^+(t) \equiv \ln \left(\frac{\varphi^+(t)}{\langle \varphi \rangle} \right) \tag{71}$$

is close to Gaussian. Figure 19 shows that the kurtosis of χ^+ is remarkably close to the Gaussian value of 3 over the large range of Reynolds numbers investigated. Furthermore, the autocorrelation function of $\chi^+(t)$, shown in Fig. 20, is well approximated by an exponential. It is thus natural to model $\chi^+(t)$ as an Ornstein–Uhlenbeck process, governed by a linear SDE similar to the Langevin equation.

Let $\sigma_a(\chi)$ denote the standard deviation of the acceleration $a^+(t)$ conditioned on $\chi^+(t)=\chi$. The DNS data⁷³ show, as expected, that $\sigma_a(\chi)$ increases steeply with χ . The conditionally standardized acceleration $\hat{a}(t)$ is defined by

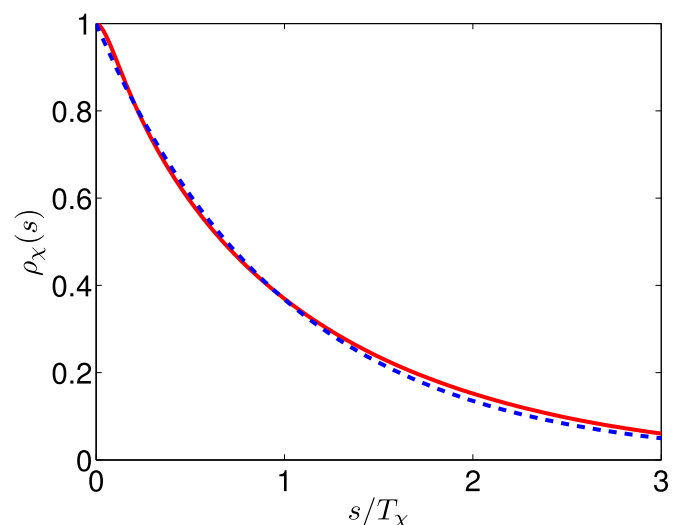


FIG. 20. (Color online) Autocorrelation function of χ , the logarithm of pseudodissipation, obtained from DNS (Ref. 77) compared to the exponential (dashed line).

$$\hat{a}(t) \equiv \frac{a^+(t)}{\sigma_a[\chi^+(t)]}. \quad (72)$$

The fact that the PDFs of conditional acceleration collapse in Fig. 18 indicates that the one-time PDF of $\hat{a}(t)$ is independent of $\chi^+(t)$ and is that observed in the figure. An empirical finding is that this PDF is well approximated by a ‘‘cubic Gaussian.’’ That is, the PDF of $\hat{a}(t)$ is well approximated by that of

$$\tilde{a} \equiv (1-p)\bar{a} + p\bar{a}^3, \quad (73)$$

where \bar{a} is a Gaussian random variable and $p=0.1$.

Based on the above observations, Lamorgese *et al.*⁸ proposed a stochastic model for velocity $u^+(t)$, acceleration $a^+(t)$, and pseudodissipation $\varphi^+(t)$, which, by construction, yields the correct one-time joint PDF of these quantities, thus appropriately accounting for internal intermittency.

E. Further stochastic Lagrangian models

Without attempting a comprehensive review, we mention here some further stochastic Lagrangian models that have been developed. For velocity and acceleration, the models described above focus on the small time scales. For inhomogeneous flows, of more importance is the effect of mean velocity gradients. The generalized Langevin model (GLM) (Ref. 78) accounts for these effects by making the drift term in the Langevin equation for the velocity vector depend linearly on the mean velocity gradient tensor. There is a correspondence between the tensor drift coefficient and models for the pressure-rate-of-strain tensor in Reynolds-stress models.²¹ In a similar manner, Sawford’s acceleration model can be generalized to incorporate the effects of mean velocity gradients.⁷⁹

The GLM models (in part) the ‘‘rapid’’ pressure, and it is consistent with rapid distortion theory to the limited extent that it correctly represents the initial response of isotropic turbulence. The stochastic wave-vector model⁸⁰ introduces a unit wavenumber vector $\mathbf{e}^+(t)$ as an additional particle property. Coupled equations for $\mathbf{u}^+(t)$ and $\mathbf{e}^+(t)$ are then constructed using a mathematical analogy to the Navier–Stokes equations in wavenumber space such that the Reynolds-stress evolution is correct for all rapid distortions of homogeneous turbulence. It is interesting to note that this exact treatment of rapid distortion is possible through stochastic modeling, but it cannot be achieved in moment closures.

Other quantities and processes related to turbulent velocity fields for which stochastic Lagrangian models have been constructed include the velocity gradient tensor,^{81–83} two-particle dispersion,^{84–87} and inertial particles.^{88–90} Some recent reviews are provided by Meneveau⁹¹ and Sawford and Pinton.¹⁸

Above we have described the IEM and IECM models which model the evolution of the composition $\phi^+(t)$ of a fluid particle due to molecular diffusion. Such ‘‘mixing models’’ are central to PDF methods for turbulent reactive flows. Arguably, this general problem is much more challenging

than modeling the velocity and related quantities. Some reasons for these challenges (not all independent) are the following:

- (1) In the conservation equation for compositions, there is no term analogous to the pressure gradient that appears in the velocity equation, and which has a randomizing effect.
- (2) Mixing occurs predominantly at the smallest scales, whereas the particle composition (or, equivalently, the one-point joint PDF of composition) contains no scale information, but is dominated by the large scales.
- (3) Different compositions can have different diffusivities, leading to differential diffusion effects, including thermal-diffusive instabilities.
- (4) Individual compositions (e.g., species mass fractions) are bounded (i.e., between 0 and 1), and sets of compositions with equal diffusivities satisfy joint boundedness conditions.
- (5) Sets of compositions with equal diffusivities satisfy linearity and independence conditions,⁹² to which models should adhere.
- (6) In reacting flows (especially premixed turbulent combustion in the flamelet regime) the steepest composition gradients can be caused by reaction fronts, rather than by turbulent straining.

Over the past 30 years, several models have been developed based solely on particle composition. These include the modified Curl model,^{93,94} the binomial Langevin model,⁹⁵ the mapping closure,^{96,97} the Euclidean minimum spanning tree (EMST) model,⁵⁷ and multiple mapping conditioning.⁵⁹

It is natural to attempt to improve the description of the physics of mixing by incorporating scale information. It has proved difficult to do so in a way that leads to a tractable model for inhomogeneous reactive flows. Some attempts have been based on composition gradients,⁹⁸ and on spectral representations,⁵⁸ including combining PDF methods with the eddy-damped quasi-normal Markovian (EDQNM) approach.⁹⁹

V. CONCLUSIONS AND FUTURE CHALLENGES

In this paper, we have illustrated the potency and broad applicability of stochastic Lagrangian models of turbulence. Dispersion from a line source in grid turbulence is a fundamental flow in the study of turbulent transport and mixing. Turbulent diffusion models (e.g., based on the k - ε model) are qualitatively incorrect, except far from the source. In contrast, the simple Langevin model for the fluid-particle velocity and the IECM model for composition yield accurate predictions of the mean, variances, and covariances from single and multiple line sources.

In Sec. III, it is shown that with straightforward extensions, these simple stochastic Lagrangian models for velocity and composition can be used to effect a turbulence closure, in terms of the joint PDF of velocity and composition, and the stochastic models form the basis for a natural particle/mesh numerical method to solve the modeled PDF equation. These PDF methods have been applied to several turbulent

flames, and they have proved most successful in accounting for important turbulence-chemistry interactions.

With the advent of DNS and modern diagnostics, it has been possible to examine in detail Lagrangian time series in turbulent flows. This examination has shown that the simple Langevin model has several limitations and deficiencies. All of these can be remedied, but at the cost of more complexity. For example, a model for velocity, acceleration, and pseudo-dissipation is able to describe accurately the Lagrangian velocity on all time scales, including Reynolds-number effects and internal intermittency.

Looking to the future, there are of course enumerable opportunities and challenges for the further development of modeling and simulation methodologies for turbulent flows. We mention here just two of these, in the context of stochastic Lagrangian modeling in conjunction with LES.

First, in a LES of a high-Reynolds-number turbulent flow, there is a significant separation of scale between the smallest scales in the flow and the smallest scales resolved in the LES. As discussed in Sec. IV E, it remains a challenge to model small-scale processes such as molecular mixing, especially when processes on these small scales are rate limiting, or when they create (rather than dissipate) fluctuations. High-Reynolds-number DNS now provides the information needed to develop and test such models.

Second, while LES provides significant modeling advantages over Reynolds-averaged Navier–Stokes (RANS) approaches, it has several problematic aspects.¹⁰⁰ In a RANS calculation, numerical errors can be quantified and reduced below acceptable levels. On the other hand, in LES as it is generally practiced, the calculated statistics depend both on the numerical method and on the grid used. A worthwhile challenge for future research is the development of a LES methodology which yields calculations with controllably small numerical effects. Such a methodology most likely requires adaptive mesh refinement and calculations on multiple grids.

ACKNOWLEDGMENTS

This paper is based on the Otto Laporte Lecture delivered at the 62nd Annual Meeting of the American Physical Society Division of Fluid Dynamics on 22 November 2009, following the award of the APS Fluid Dynamics Prize. I would like to thank all my current and former students, post-docs, and collaborators who have contributed to the body of research described here. I am particularly grateful to Brian Sawford, Haifeng Wang, Sharadha Viswanathan, Zellman Warhaft, and P. K. Yeung who have directly contributed to the paper. This work is supported in part by Air Force Office of Scientific Research under Grant No. FA-9550-09-1-0047 and in part by the Department of Energy under Grant No. DE-FG02-90ER14128.

¹A. N. Kolmogorov, “The local structure of turbulence in incompressible viscous fluid for very large Reynolds numbers,” *Dokl. Akad. Nauk SSSR* **30**, 299 (1941).

²P. Langevin, “Sur la théorie du mouvement Brownien,” *Acad. Sci., Paris, C. R.* **146**, 530 (1908).

³G. I. Taylor, “Diffusion by continuous movements,” *Proc. London Math. Soc.* **20**, 196 (1921).

⁴M. S. Anand and S. B. Pope, in *Turbulent Shear Flows 4*, edited by L. J. S. Bradbury, F. Durst, B. E. Launder, F. W. Schmidt, and J. H. Whitelaw (Springer-Verlag, Berlin, 1985), pp. 46–61.

⁵B. L. Sawford, “Micro-mixing modelling of scalar fluctuations in plumes in homogeneous turbulence,” *Flow, Turbul. Combust.* **72**, 133 (2004).

⁶S. Viswanathan and S. B. Pope, “Turbulent dispersion behind line sources in grid turbulence,” *Phys. Fluids* **20**, 101514 (2008).

⁷B. L. Sawford, “Reynolds number effects in Lagrangian stochastic models of turbulent dispersion,” *Phys. Fluids A* **3**, 1577 (1991).

⁸A. G. Lamorgese, S. B. Pope, P. K. Yeung, and B. L. Sawford, “A conditionally cubic-Gaussian stochastic Lagrangian model for acceleration in isotropic turbulence,” *J. Fluid Mech.* **582**, 423 (2007).

⁹M. S. Uberoi and S. Corrsin, “Diffusion of heat from a line source in isotropic turbulence,” National Aeronautics and Space Administration Report No. 1142, 1953.

¹⁰A. A. Townsend, “The diffusion behind a line source in homogeneous turbulence,” *Proc. R. Soc. London, Ser. A* **224**, 487 (1954).

¹¹Z. Warhaft, “The interference of thermal fields from line sources in grid turbulence,” *J. Fluid Mech.* **144**, 363 (1984).

¹²H. Stapountzis, B. L. Sawford, J. C. R. Hunt, and R. E. Britter, “Structure of the temperature field downwind of a line source in grid turbulence,” *J. Fluid Mech.* **165**, 401 (1986).

¹³B. L. Sawford and C. M. Tivendale, “Measurements of concentration statistics downstream of a line source in grid turbulence,” *Proceedings of the 11th Australasian Fluid Mechanics Conference* (University of Tasmania, Hobart, 1992), pp. 945–948.

¹⁴W. P. Jones and B. E. Launder, “The prediction of laminarization with a two-equation model of turbulence,” *Int. J. Heat Mass Transfer* **15**, 301 (1972).

¹⁵P. K. Yeung and S. B. Pope, “Lagrangian statistics from direct numerical simulations of isotropic turbulence,” *J. Fluid Mech.* **207**, 531 (1989).

¹⁶S. B. Pope, *Turbulent Flows* (Cambridge University Press, Cambridge, 2000).

¹⁷A. N. Kolmogorov, “A refinement of previous hypotheses concerning the local structure of turbulence in a viscous incompressible fluid at high Reynolds number,” *J. Fluid Mech.* **13**, 82 (1962).

¹⁸B. L. Sawford and J.-F. Pinton, in *The Nature of Turbulence*, edited by P. A. Davidson, Y. Kaneda, and K. R. Sreenivasan (Cambridge University Press, Cambridge, 2011).

¹⁹J. Villermaux and J. C. Devillon, “Représentation de la coalescence et de la redispersion des domaines de ségrégation dans un fluide par un modèle d’interaction phénoménologique,” *Proceedings of the Second International Symposium on Chemical Reaction Engineering* (Elsevier, New York, 1972), pp. 1–13.

²⁰C. Dopazo and E. E. O’Brien, “An approach to the autoignition of a turbulent mixture,” *Acta Astronaut.* **1**, 1239 (1974).

²¹S. B. Pope, “On the relationship between stochastic Lagrangian models of turbulence and second-moment closures,” *Phys. Fluids* **6**, 973 (1994).

²²R. O. Fox, “On velocity-conditioned scalar mixing in homogeneous turbulence,” *Phys. Fluids* **8**, 2678 (1996).

²³S. B. Pope, “The vanishing effect of molecular diffusivity on turbulent dispersion: Implications for turbulent mixing and the scalar flux,” *J. Fluid Mech.* **359**, 299 (1998).

²⁴O. Reynolds, “On the dynamical theory of incompressible viscous flows and the determination of the criterion,” *Philos. Trans. R. Soc. London, Ser. A* **186**, 123 (1894).

²⁵S. B. Pope, “PDF methods for turbulent reactive flows,” *Prog. Energy Combust. Sci.* **11**, 119 (1985).

²⁶D. C. Haworth, “Progress in probability density function methods for turbulent reacting flows,” *Prog. Energy Combust. Sci.* **36**, 168 (2010).

²⁷B. J. Delarue and S. B. Pope, “Application of PDF methods to compressible turbulent flows,” *Phys. Fluids* **9**, 2704 (1997).

²⁸P. R. Van Slooten, Jayesh, and S. B. Pope, “Advances in PDF modeling for inhomogeneous turbulent flows,” *Phys. Fluids* **10**, 246 (1998).

²⁹M. Muradoglu, P. Jenny, S. B. Pope, and D. A. Caughey, “A consistent hybrid finite-volume/particle method for the PDF equations of turbulent reactive flows,” *J. Comput. Phys.* **154**, 342 (1999).

³⁰S. B. Pope, “A Monte Carlo method for the PDF equations of turbulent reactive flow,” *Combust. Sci. Technol.* **25**, 159 (1981).

³¹L. Valiño, “A field Monte Carlo formulation for calculating the probability density function of a single scalar in a turbulent flow,” *Flow, Turbul. Combust.* **60**, 157 (1998).

³²V. A. Sabel’nikov and O. Soulard, “Rapidly decorrelating velocity-field model as a tool for solving one-point Fokker-Planck equations for prob-

- ability density functions of turbulent reactive scalars," *Phys. Rev. E* **72**, 016301 (2005).
- ³³R. O. Fox, *Computational Models for Turbulent Reactive Flows* (Cambridge University Press, New York, 2003).
- ³⁴R. McDermott and S. B. Pope, "The parabolic edge reconstruction method (PERM) for Lagrangian particle advection," *J. Comput. Phys.* **227**, 5447 (2008).
- ³⁵J. Xu and S. B. Pope, "PDF calculations of turbulent nonpremixed flames with local extinction," *Combust. Flame* **123**, 281 (2000).
- ³⁶R. Cao and S. B. Pope, "The influence of chemical mechanisms on PDF calculations of nonpremixed piloted jet flames," *Combust. Flame* **143**, 450 (2005).
- ³⁷R. S. Barlow and J. H. Frank, "Effects of turbulence on species mass fraction in methane/air jet flames," *Proc. Combust. Inst.* **27**, 1087 (1998).
- ³⁸R. Cabra, T. Myhrvold, J. Y. Chen, R. W. Dibble, A. N. Karpetis, and R. S. Barlow, "Simultaneous laser Raman-Rayleigh-LIF measurements and numerical modeling results of a lifted turbulent H₂/N₂ jet flame in a vitiated coflow," *Proc. Combust. Inst.* **29**, 1881 (2002).
- ³⁹Z. Wu, S. H. Starner, and R. W. Bilger, "Lift-off heights of turbulent H₂/N₂ jet flames in a vitiated coflow," in *Proceedings of the 2003 Australian Symposium on Combustion and the Eighth Australian Flame Days*, edited by D. Honnery (Monash University, Victoria, 2003).
- ⁴⁰R. L. Gordon, S. H. Starner, A. R. Masri, and R. W. Bilger, "Further characterisation of lifted hydrogen and methane flames issuing into a vitiated coflow," *Proceedings of the Fifth Asia-Pacific Conference on Combustion*, 2005.
- ⁴¹R. Cao, S. B. Pope, and A. R. Masri, "Turbulent lifted flames in a vitiated coflow investigated using joint PDF calculations," *Combust. Flame* **142**, 438 (2005).
- ⁴²H. Wang and S. B. Pope, "Lagrangian investigation of local extinction, re-ignition and auto-ignition in turbulent flames," *Combust. Theory Modell.* **12**, 857 (2008).
- ⁴³J. Li, Z. Zhao, A. Kazakov, and F. L. Dryer, "An updated comprehensive kinetic model for H₂ combustion," Technical Report, Fall Technical Meeting of the Eastern States Section of the Combustion Institute, Penn State University, University Park, PA, 2003.
- ⁴⁴R. L. Gordon, A. R. Masri, S. B. Pope, and G. M. Goldin, "A numerical study of auto-ignition in turbulent lifted flames issuing into a vitiated coflow," *Combust. Theory Modell.* **11**, 351 (2007).
- ⁴⁵C. S. Yoo, R. Sankaran, and J. H. Chen, "Three-dimensional direct numerical simulation of a turbulent lifted hydrogen jet flame in heated coflow: Flame stabilization and structure," *J. Fluid Mech.* **640**, 453 (2009).
- ⁴⁶S. B. Pope, "Computations of turbulent combustion: Progress and challenges," *Proc. Combust. Inst.* **23**, 591 (1990).
- ⁴⁷F. Gao and E. E. O'Brien, "A large-eddy simulation scheme for turbulent reacting flows," *Phys. Fluids A* **5**, 1282 (1993).
- ⁴⁸P. J. Colucci, F. A. Jaber, P. Givi, and S. B. Pope, "Filtered density function for large eddy simulation of turbulent reacting flows," *Phys. Fluids* **10**, 499 (1998).
- ⁴⁹S. B. Pope, "Self-conditioned fields for large-eddy simulations of turbulent flows," *J. Fluid Mech.* **652**, 139 (2010).
- ⁵⁰P. Givi, "Filtered density function for subgrid scale modeling of turbulent combustion," *AIAA J.* **44**, 16 (2006).
- ⁵¹S. James, J. Zhu, and M. S. Anand, "Large eddy simulations of turbulent flames using the filtered density function model," *Proc. Combust. Inst.* **31**, 1737 (2007).
- ⁵²H. Pitsch, "Large-eddy simulation of turbulent combustion," *Annu. Rev. Fluid Mech.* **38**, 453 (2006).
- ⁵³D. C. Haworth and S. B. Pope, "Transported probability density function methods for Reynolds-averaged and large-eddy simulations," *Turbulent Combustion* (Springer, Dordrecht/Hedielberg/London/New York, 2011).
- ⁵⁴H. Wang and S. B. Pope, "Large eddy simulation/probability density function modeling of a turbulent CH₄/H₂/N₂ jet flame," *Proc. Combust. Inst.* **33**, 1319 (2011).
- ⁵⁵W. P. Jones and V. N. Prasad, "Large eddy simulation of the Sandia flame series (D-F) using the Eulerian stochastic field method," *Combust. Flame* **157**, 1621 (2010).
- ⁵⁶H. Koo, P. Donde, and V. Raman, "A quadrature-based LES/transported probability density function approach for modeling supersonic combustion," *Proc. Combust. Inst.* **33**, 2203 (2011).
- ⁵⁷S. Subramaniam and S. B. Pope, "A mixing model for turbulent reactive flows based on Euclidean minimum spanning trees," *Combust. Flame* **115**, 487 (1998).
- ⁵⁸R. O. Fox, "The Lagrangian spectral relaxation model of the scalar dissipation in homogeneous turbulence," *Phys. Fluids* **9**, 2364 (1997).
- ⁵⁹A. Y. Klimenko and S. B. Pope, "A model for turbulent reactive flows based on multiple mapping conditioning," *Phys. Fluids* **15**, 1907 (2003).
- ⁶⁰S. B. Pope and M. S. Anand, "Flamelet and distributed combustion in premixed turbulent flames," *Proc. Combust. Inst.* **20**, 403 (1985).
- ⁶¹R. P. Lindstedt and E. M. Vaos, "Transported PDF modeling of high-Reynolds-number premixed turbulent flames," *Combust. Flame* **145**, 495 (2006).
- ⁶²K. A. Kemenov and S. B. Pope, "Molecular diffusion effects in LES of a piloted methane-air flame," *Combust. Flame* **157**, 240 (2011).
- ⁶³Y. Kaneda and T. Gotoh, "Lagrangian velocity autocorrelation in isotropic turbulence," *Phys. Fluids A* **3**, 1924 (1991).
- ⁶⁴Y. Kimura and J. R. Herring, "Diffusion in stably stratified turbulence," *J. Fluid Mech.* **328**, 253 (1996).
- ⁶⁵L. Biferale, G. Boffetta, A. Celani, A. Lanotte, and F. Toschi, "Particle trapping in three-dimensional fully developed turbulence," *Phys. Fluids* **17**, 021701 (2005).
- ⁶⁶G. A. Voth, K. Satyanarayan, and E. Bodenschatz, "Lagrangian acceleration measurements at large Reynolds number," *Phys. Fluids* **10**, 2268 (1998).
- ⁶⁷S. Ott and J. Mann, "An experimental investigation of the relative diffusion of particle pairs in three-dimensional turbulent flow," *J. Fluid Mech.* **422**, 207 (2000).
- ⁶⁸G. A. Voth, A. LaPorta, A. M. Crawford, J. Alexander, and E. Bodenschatz, "Measurement of particle accelerations in fully developed turbulence," *J. Fluid Mech.* **469**, 121 (2002).
- ⁶⁹N. Mordant, P. Metz, O. Michel, and J.-F. Pinton, "Measurement of Lagrangian velocity in fully developed turbulence," *Phys. Rev. Lett.* **87**, 214501 (2001).
- ⁷⁰P. K. Yeung, S. B. Pope, and B. L. Sawford, "Reynolds number dependence of Lagrangian statistics in large numerical simulations of isotropic turbulence," *J. Turbul.* **7**, 58 (2006).
- ⁷¹B. L. Sawford, P. K. Yeung, and J. F. Hackl, "Reynolds number dependence of relative dispersion statistics in isotropic turbulence," *Phys. Fluids* **20**, 065111 (2008).
- ⁷²N. Mordant, A. M. Crawford, and E. Bodenschatz, "Experimental Lagrangian acceleration probability density function measurement," *Physica D* **193**, 245 (2004).
- ⁷³P. K. Yeung, S. B. Pope, A. G. Lamorgese, and D. A. Donzis, "Acceleration and dissipation statistics in numerical simulations of isotropic turbulence," *Phys. Fluids* **18**, 065103 (2006).
- ⁷⁴A. M. Oboukhov, "Some specific features of atmospheric turbulence," *J. Fluid Mech.* **13**, 77 (1962).
- ⁷⁵S. B. Pope and Y. L. Chen, "The velocity-dissipation probability density function model for turbulent flows," *Phys. Fluids A* **2**, 1437 (1990).
- ⁷⁶A. M. Reynolds, "Superstatistical mechanics of tracer-particle motions in turbulence," *Phys. Rev. Lett.* **91**, 084503 (2003).
- ⁷⁷P. K. Yeung, S. B. Pope, E. A. Kurth, and A. G. Lamorgese, "Lagrangian conditional statistics, acceleration and local relative motion in numerically simulated isotropic turbulence," *J. Fluid Mech.* **582**, 399 (2007).
- ⁷⁸D. C. Haworth and S. B. Pope, "A generalized Langevin model for turbulent flows," *Phys. Fluids* **29**, 387 (1986).
- ⁷⁹S. B. Pope, "A stochastic Lagrangian model for acceleration in turbulent flows," *Phys. Fluids* **14**, 2360 (2002).
- ⁸⁰P. R. Van Sooten and S. B. Pope, "PDF modeling of inhomogeneous turbulence with exact representation of rapid distortions," *Phys. Fluids* **9**, 1085 (1997).
- ⁸¹S. S. Girimaji and S. B. Pope, "A stochastic model for velocity gradients in turbulence," *Phys. Fluids A* **2**, 242 (1990).
- ⁸²J. Martín, C. Dopazo, and L. Valiño, "Dynamics of velocity gradient invariants in turbulence: Restricted Euler and linear diffusion models," *Phys. Fluids* **10**, 2012 (1998).
- ⁸³L. Chevillard and C. Meneveau, "Intermittency and universality in a Lagrangian model of velocity gradients in three-dimensional turbulence," *C. R. Mec.* **335**, 187 (2007).
- ⁸⁴P. A. Durbin, "A stochastic model of two-particle dispersion and concentration fluctuations in homogeneous turbulence," *J. Fluid Mech.* **100**, 279 (1980).
- ⁸⁵D. J. Thomson, "A stochastic model for the motion of particle pairs in isotropic high-Reynolds-number turbulence, and its application to the problem of concentration variance," *J. Fluid Mech.* **210**, 113 (1990).
- ⁸⁶M. S. Borgas and B. L. Sawford, "A family of stochastic models for two-particle dispersion in isotropic, homogeneous and stationary turbulence," *J. Fluid Mech.* **279**, 69 (1994).

- ⁸⁷M. S. Borgas and P. K. Yeung, "Relative dispersion in isotropic turbulence. Part 2. A new stochastic model with Reynolds-number dependence," *J. Fluid Mech.* **503**, 125 (2004).
- ⁸⁸B. L. Sawford and F. M. Guest, "Lagrangian statistical simulation of the turbulent motion of heavy-particles," *Boundary-Layer Meteorol.* **54**, 147 (1991).
- ⁸⁹M. Guingo and J. P. Minier, "A stochastic model of coherent structures for particle deposition in turbulent flows," *Phys. Fluids* **20**, 053303 (2008).
- ⁹⁰I. Fouxon and P. Horvai, "Separation of heavy particles in turbulence," *Phys. Rev. Lett.* **100**, 040601 (2008).
- ⁹¹C. Meneveau, "Lagrangian dynamics and models of the velocity gradient tensor in turbulent flows," *Annu. Rev. Fluid Mech.* **43**, 219 (2011).
- ⁹²S. B. Pope, "Consistent modeling of scalars in turbulent flows," *Phys. Fluids* **26**, 404 (1983).
- ⁹³R. L. Curl, "Dispersed phase mixing. I," *AIChE J.* **9**, 175 (1963).
- ⁹⁴J. Janicka, W. Kolbe, and W. Kollmann, "Closure of the transport equation for the probability density function of turbulent scalar fields," *J. Non-Equilib. Thermodyn.* **4**, 47 (1977).
- ⁹⁵L. Valiño and C. Dopazo, "A binomial Langevin model for turbulent mixing," *Phys. Fluids A* **3**, 3034 (1991).
- ⁹⁶H. Chen, S. Chen, and R. H. Kraichnan, "Probability distribution of a stochastically advected scalar field," *Phys. Rev. Lett.* **63**, 2657 (1989).
- ⁹⁷S. B. Pope, "Mapping closures for turbulent mixing and reaction," *Theor. Comput. Fluid Dyn.* **2**, 255 (1991).
- ⁹⁸J. Martín, C. Dopazo, and L. Valiño, "Joint statistics of the scalar gradient and the velocity gradient in turbulence using linear diffusion models," *Phys. Fluids* **17**, 028101 (2005).
- ⁹⁹Y. Xia, Y. Liu, T. Vaithianathan, and L. R. Collins, "Eddy damped quasi normal Markovian theory for chemically reactive scalars in isotropic turbulence," *Phys. Fluids* **22**, 045103 (2010).
- ¹⁰⁰S. B. Pope, "Ten questions concerning the large-eddy simulation of turbulent flows," *New J. Phys.* **6**, 35 (2004).